Renormalization group functional equations

Thomas L. Curtright and Cosmas K. Zachos

Phys. Rev. D **83**, 065019 — Published 16 March 2011

DOI: 10.1103/PhysRevD.83.065019

ANL-HEP-PR-10-52, CERN-PH-TH-2010-245

Renormalization Group Functional Equations

Thomas L. Curtright[1,2] and Cosmas K. Zachos[3]

[1]*CERN, CH-1211 Geneva 23, Switzerland*

[2]*Department of Physics, University of Miami, Coral Gables, FL 33124-8046, USA*

[3]*High Energy Physics Division, Argonne National Laboratory, Argonne, IL 60439-4815, USA*

Abstract

Functional conjugation methods are used to analyze the global structure of various renormalization group trajectories, and to gain insight into the interplay between continuous and discrete rescaling. With minimal assumptions, the methods produce continuous flows from step-scaling σ functions, and lead to exact functional relations for the local flow β functions, whose solutions may have novel, exotic features, including multiple branches. As a result, fixed points of σ are sometimes *not* true fixed points under continuous changes in scale, and zeroes of β do *not* necessarily signal fixed points of the flow, but instead may only indicate turning points of the trajectories.

I. INTRODUCTION

The renormalization group (RG) of Gell-Mann and Low [14], and of Stueckelberg and Petermann [24], has an elegant mathematical expression in terms of the functional conjugation (FC) methods of Ernst Schröder [23]. This expression provides a powerful tool to describe the behavior of physical systems under either infinitesimal or finite, perhaps large, changes in scale. While this fact is often overlooked, and not usually invoked in the solution of various problems posed in the RG framework, it is readily apparent upon reading [14] (see especially Appendix B; also see [19]) and surveying the literature on functional equations [16]. Moreover, it may be profitable to bear in mind the logical connections between these two subjects when considering the step-scaling approach in lattice gauge theory [4, 20], where the power and utility of the methods are manifest.

In previous work [7–9] we have discussed how dynamical systems, defined on a discrete lattice of time points, may be smoothly interpolated in time through the use of solutions to Schröder's celebrated functional equation. Here we discuss the same methods in the context of the renormalization group. We examine in detail the connections between differential (local) rescaling and finite (global) changes in scale. We interpolate various step-scaling functions to obtain trajectories under continuous change of scale, with emphasis on the consistency imposed by the analytic properties of couplings in the presence of UV and IR fixed points. From this point of view it is possible to obtain novel features for RG behavior. In particular, multi-valued Callan–Symanzik β functions [3, 14, 24, 25] are commonly encountered in the local RG flow equations, even when interpolating elementary, polynomial step-scaling functions, with interesting consequences involving fixed points, cycles, and even chaotic evolution under changes in scale.

In section II we describe functional conjugation methods relevant to RG analysis and apply them to the study of selected trajectories. In section III we consider a physical illustration of fixed point behavior drawn from numerical studies of lattice gauge theory [1]. In section IV we illustrate elementary limit cycle behavior in a model obtained by an extension of the standard BCS Hamiltonian [17]. In section V we briefly explain how further novel, exotic features can arise from basic step-scaling behavior, in general. Finally, in section VI we exhibit such features, including multi-valued β functions, limit cycles, and chaotic trajectories, using toy models based on the logistic map. Two appendices provide

some connections to our earlier work on dynamical systems, and a few algebraic details for the lattice example.

II. METHODOLOGY

A. The renormalization group: Step by step

Let us suppose the change in the coupling u is given for a discrete change in length scale by

$$u \mapsto \sigma(u) \ , \tag{1}$$

where $\sigma(u)$ is the "step-scaling" function [4, 20]. Typically, $u = g^2/4\pi$, where g is the gauge coupling, although it may be convenient to incorporate other numerical factors into u, or even to take other functions of g^2, depending on the problem at hand. The standard interpretation is to regard $\sigma(u)$ as a discrete Δt sampling of a renormalization trajectory, $u(t)$, whose continuous evolution under changes in the *log* of the length scale, t, has proceeded from an initial $u \equiv u(t)|_{t=0}$. This notation for the initial u (rather than u_0, say) is not only more convenient to express the step-scaling function, e.g. as the mapping (1), but also to write many relations that hold both for the initial u as well as more generally for all $u(t)$. We will point out several such relations in the following.

The trajectory is assumed to describe an abelian t-flow with group composition given by simple addition of t arguments. So, for example, $\sigma(u) = u(t)|_{t=1}$, $\sigma(\sigma(u)) = u(t)|_{t=2}$, $\sigma^{-1}(u) = u(t)|_{t=-1}$, etc. The local flow equation in terms of t has both familiar and more recondite forms,

$$\frac{du}{dt} = \beta(u) \equiv (\ln\lambda)\,\Psi(u)/\Psi'(u)\,, \tag{2}$$

where β is the so-called Callan-Symanzik function [3, 25] (which appeared earlier in [24], Eq(4.25), under the alias $h_{i\rho}$) and Ψ is the so-called Schröder function [23] (both of which appeared in [14], under the aliases ψ and G, respectively), and where $1/\ln\lambda$ (usually taken to be ± 1) sets the scale of t. It is also implicitly understood that the system is underlain by a t-translation covariance so that (2) holds not just for $u \equiv u(t)|_{t=0}$ but also for $u(t)$, provided of course that the RHS is also modified by $\beta(u) \to \beta(u(t))$ and $\Psi(u) \to \Psi(u(t))$.

While the Schröder function is less well-known in renormalization theory, it is immediately

expressed in terms of β from the definition in (2), rewritten as

$$d \ln \Psi(u) / du = (\ln \lambda) / \beta(u) \ . \tag{3}$$

Thus a definite integral gives the total change in Ψ brought about by a finite change in the coupling,

$$\Psi(u_2) = \lambda^{\int_{u_1}^{u_2} \frac{du}{\beta(u)}} \ \Psi(u_1) \ . \tag{4}$$

On the other hand, the exponent here is just $t_2 - t_1$, the total change in t as $u_1 \to u_2$, as follows from the first equality in (2). Therefore another way to express (4) is in terms of the evolution of the Schröder function under the flow of the coupling, $u \to u(t)$,

$$\Psi(u(t)) = \lambda^t \ \Psi(u) \ . \tag{5}$$

This last relation reveals the fundamental role played by Ψ, and its inverse function Ψ^{-1}, in the construction of trajectories for arbitrary changes in t. It follows from (5) that such *global flow* is given by [14]

$$u(t) = \Psi^{-1}\left(\lambda^t \Psi(u)\right) \ , \tag{6}$$

where $1/\ln\lambda$ sets the scale of t. The RHS of (6) is immediately recognized as just a change of variable, effected through a functional conjugation [23]. For us, in fact, the expression "Schröder functional method" is just a metonymy for *functional conjugation*.

Indeed, the expression (6) is perhaps the most succinct way to appreciate that renormalization relates self-similar structures at different scales, inasmuch as the RHS is just a functional similarity transformation: $\Psi^{-1} \circ \lambda^t \circ \Psi$.

Moreover, (6) shows that fixed points or limit cycles can arise in a model for real λ if and only if Ψ^{-1} either becomes constant or else exhibits periodic behavior, respectively.

The structure of (6) also makes the abelian t-flow of the renormalization group manifest, and it gives a formula for the step-scaling function, or any of its functional compositions, in terms of Ψ. For example, for $\sigma(u) \equiv u(t)|_{t=1}$, we have from (5)

$$\lambda \Psi(u) = \Psi(\sigma(u)) \ , \tag{7}$$

a form known as "Schröder's functional equation with eigenvalue λ." Presented in this form, for a given $\sigma(u)$, the problem is often to determine all allowed λ and to find all solutions of the functional equation [29].

Alternatively, we may write (7) as

$$\sigma(u) = \Psi^{-1}(\lambda \Psi(u)) \ . \tag{8}$$

In this form, the equation determines the step-scaling function in terms of Ψ. In fact, it is useful to think of $u(t)$ in (6) as $\sigma_t(u)$, that is, as a t-th *continuous* functional composition of σ. For example, $\sigma_2(u) = \sigma(\sigma(u))$ as before, but now generalized to $\sigma(u) = \sigma_{1/2}\left(\sigma_{1/2}(u)\right)$, etc. More generally, $\sigma_{t_1+t_2}(u) = \sigma_{t_1}(\sigma_{t_2}(u))$ — just the expected RG abelian composition rule.

At this point it is natural to ask, what is a simple physical model whereby $\Psi(t) = \lambda^t \Psi_0$? Well, $d \ln \Psi(t)/dt = \ln \lambda$, so clearly $\ln \Psi$ is the variable of choice. Then the question becomes, for what model is the change in the coupling with scale a constant? An obvious answer is, *the one-loop approximation* for evolution of an inverted coupling, $1/\mathfrak{g}^2$. That is to say, if

$$\frac{d}{dt}\mathfrak{g}(t) = \beta_{\mathfrak{g}\ \text{1-loop}} = \frac{1}{2}\mathfrak{c}\mathfrak{g}^3(t) \ , \tag{9}$$

then

$$\frac{d}{dt}\left(\frac{1}{\mathfrak{g}^2(t)}\right) = -\mathfrak{c} \ . \tag{10}$$

So, the physical interpretation of the Schröder function is clear: The log of Ψ is just the change of variable needed to convert the renormalization group flow for u into a one-loop flow for a re-defined coupling constant $1/\mathfrak{g}^2$. Thus,

$$\frac{d}{dt}\ln \Psi(u(t)) = \ln \lambda \quad \Longleftrightarrow \quad \frac{d}{dt}\left(\frac{1}{\mathfrak{g}^2(t)}\right) = -\mathfrak{c} \ . \tag{11}$$

The role of $\ln \Psi$ is put into deeper perspective through the following formal sequence of steps that evoke the method of characteristics for the RG. Making explicit the dependence of the trajectory on the initial $u = u(t)|_{t=0}$ as well as on t, and making use of

$$\frac{\partial}{\partial t} = \beta(u)\frac{\partial}{\partial u} = (\ln \lambda)\frac{\partial}{\partial \ln \Psi(u)} \tag{12}$$

along the trajectory, we have

$$u(t,u) = e^{t\frac{\partial}{\partial \tau}}\ u(\tau,u)\Big|_{\tau=0} = e^{t\beta(u)\frac{\partial}{\partial u}}\ u = e^{t(\ln\lambda)\frac{\partial}{\partial \ln \Psi(u)}}\ u \ . \tag{13}$$

But now, $u = \Psi^{-1}(\Psi(u)) = \Psi^{-1}(\exp(\ln \Psi(u)))$, so the last expression reduces to a mere translation of the variable $\ln(\Psi(u))$,

$$e^{t(\ln\lambda)\frac{\partial}{\partial \ln \Psi(u)}}\ \Psi^{-1}(\exp(\ln \Psi(u))) = \Psi^{-1}(\exp(t\ln\lambda + \ln \Psi(u))) = \Psi^{-1}\left(\lambda^t \Psi(u)\right) \ . \tag{14}$$

Thus (6) is recovered. These formal steps can be made precise by examination of T, the radius of convergence of the t series, in particular by a determination of the dependence of T on the initial u. How this goes will be illustrated in the examples to follow.

There is some additional, subtle mathematical structure to take into account here, especially if we have in hand a series expansion for σ:

$$\sigma(u) = \alpha u + O\left(u^2\right) \ . \tag{15}$$

For example, if $\frac{d}{dt}u(t) = cu^2(t)$, as is true for lowest order perturbation theory with $u \propto g^2$, then the exact solution for the trajectory is

$$u(t) = \frac{u}{1 - cut} \ , \tag{16}$$

where again on the RHS $u = u(t)|_{t=0}$. In this case we have $\alpha = 1$ in (15).

But this leads to $\lambda = 1$, the well-known singular situation for the eigenvalue in Schröder's functional equation. By singular we mean that an attempt to solve (7) by Taylor series expansion about $u = 0$ will fail, in general, when $\lambda = 1$. Indeed, it is immediately verified that, for $\alpha = 1$ in (15), a nontrivial solution of (7) can *not* be found with $\Psi(u)$ given by a series about $u = 0$.

This is easily circumvented, however. Instead of Taylor series about $u = 0$, all the relevant solutions have an essential singularity at $u = 0$, and in fact have Taylor series about $u = \infty$. Explicitly, with $\lambda \equiv \exp(\kappa c)$ in (3), we see that $\Psi_\kappa(u) = \exp\left(-\frac{\kappa}{u}\right)$ is a family of Schröder functions for one-loop evolution, with arbitrary κ: $\Psi_\kappa(u(t)) = e^{\kappa ct}\ \Psi_\kappa(u)$. So, for $t = 1$ and $\sigma(u) \equiv u(t)|_{t=1}$, the eigenvalue for each Ψ_κ solution is indeed λ, and not the naive value 1 (excluding the trivial and uninteresting case where $\Psi_{\kappa=0} = 1$). Defining a discrete step for another value of t simply rescales κ.

We will say more about the general structure of the functional approach to the RG, and the novel features that it has the power to reveal, in sections IV and V of the paper. But first, we consider:

B. The β functional equation, with one- and two-loop examples

What is the functional equation obeyed by the local β function? It follows simply enough from (2), or else from the definition in (2) combined with (7). Thus,

$$\frac{\Psi(u)}{\frac{d}{du}\Psi(u)} = \frac{\Psi(\sigma(u))}{\frac{d}{du}\Psi(\sigma(u))} = \frac{1}{\frac{d}{du}\sigma(u)}\frac{\Psi(\sigma(u))}{\Psi'(\sigma(u))} \ . \tag{17}$$

That is to say (cf. Eq (6) in [9]),

$$\beta(\sigma(u)) = \frac{d\sigma(u)}{du}\ \beta(u) \ . \tag{18}$$

This is just the flow of $\sigma(u)$ along the characteristics defined by (12). Note that all *explicit* reference to the eigenvalue λ has dropped out of this equation, although it is still possible for λ dependence to be induced through implicit λ dependence in $\sigma(u)$, and therefore λ dependence is implicitly understood for β as well. Also note that (18) alone does not determine the overall normalization of β. This normalization is determined by (2) and (7), and it also introduces λ dependence.

As an example, again take $\beta(u) = cu^2$, the one-loop result. For $t = 1$, we have $\sigma(u) = \frac{u}{1-cu}$, hence

$$\frac{d\sigma(u)}{du} = \frac{1}{(1-cu)^2} \ . \tag{19}$$

But we also have

$$\beta(\sigma(u)) = c\sigma^2(u) = \frac{cu^2}{(1-cu)^2} = \frac{1}{(1-cu)^2}\ \beta(u) \ . \tag{20}$$

So, (18) holds — the most important point to take away from this example being that a Taylor series solution about $u = 0$ *can work* for the functional equation obeyed by $\beta(u)$, even though it does *not* work for $\Psi(u)$. It is of course redundant to do so, but we check this, for $\beta(u) \equiv au + \gamma u^2 + bu^3$. Then $\sigma(u) = \frac{u}{1-cu}$ gives $\beta(\sigma(u)) - \left(\frac{d\sigma(u)}{du}\right)\beta(u) = \frac{cu^2}{(cu-1)^3}(-bu^2 - acu + a)$. For this to vanish, it is necessary and sufficient that both $a = 0$ and $b = 0$, while γ is undetermined.

1. *Two-loop infrared fixed point*

For another, more interesting example, consider the two-loop perturbative approximation to β for a model with trivial UV *and* nontrivial IR fixed points. This example nicely

illustrates how the normalization of β is determined in the functional approach. We may sweep various model dependent factors into the definition of the coupling, g, and the scale of t to write:

$$\frac{dg}{dt} = \frac{1}{2}\, g^3 \left(1 - g^2\right) \ . \tag{21}$$

Changing variable to

$$y = \frac{1}{g^2} - 1 \ , \tag{22}$$

(21) becomes

$$\frac{dy}{dt} = \frac{-y}{1+y} \ , \tag{23}$$

with solution [13]

$$y\left(t\right) = \text{LambertW}\left(y_0 e^{y_0 - t}\right) \ , \tag{24}$$

where LambertW is the inverse function for $x \exp x$. This is manifestly in FC form (6), with $\lambda = 1/e$ and $\Psi\left(y\right) = y \exp y$, where Ψ satisfies the functional equation

$$\frac{1}{e}\, \Psi\left(y\right) = \Psi\left(\text{LambertW}\left(\frac{1}{e}\, y \exp\left(y\right)\right)\right) \ . \tag{25}$$

From this, we immediately read-off the step-scaling function in terms of y. Switching back to the original coupling g the solution (24) gives

$$g^2\left(t\right) = \frac{1}{1 + \text{LambertW}\left(\left(\frac{1}{g_0^2} - 1\right) e^{-t-1+1/g_0^2}\right)} \ . \tag{26}$$

A typical trajectory is shown here.

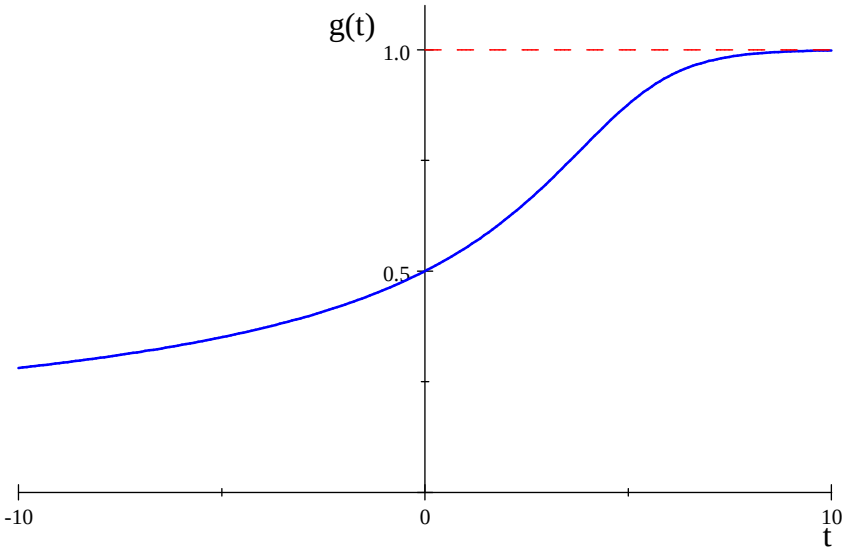

A 2-loop trajectory with $g\left(0\right) = 1/2$.

In this example, Ψ *can* be obtained by Taylor series solution of the functional equation, (25), only it is a Taylor series about the *non-trivial* fixed point at $g = 1$, i.e. $y = 0$. Nonetheless, for this two-loop example, one may forego the series solution of (25) and just solve it by inspection, upon noting that $\text{LambertW}^{-1}(z) = ze^z$.

For this same example, the β function can be obtained *from the step-scaling function* by series solution about *either* fixed point, $g = 0$ or $g = 1$. In terms of the variable y with $\sigma(y) = y(t)|_{t=1}$, we have

$$\sigma(y) = \text{LambertW}\left(\frac{1}{e}\, y \exp(y)\right) \;, \quad \frac{d\sigma(y)}{dy} = \frac{1+y}{y}\, \frac{\text{LambertW}\left(ye^{-1+y}\right)}{\left(1+\text{LambertW}\left(ye^{-1+y}\right)\right)} \;. \tag{27}$$

This leads to a typical plot of σ near the fixed point.

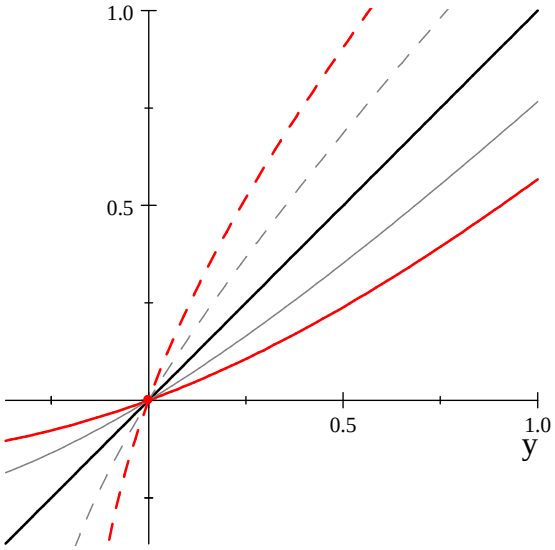

Two-loop IR fixed point exhibited by $\sigma(y)$ (solid red) and $\sigma^{-1}(y)$ (dashed red) versus y. Light gray curves are the functional square roots of σ and σ^{-1}.

Of course, with all the additional information about the actual trajectory implicitly built into this closed-form expression for σ, we may also forego an actual series solution of (18) and solve it too by inspection. Explicitly writing out the functional equation as

$$\beta\left(\text{LambertW}\left(ye^{-1+y}\right)\right) = \frac{\text{LambertW}\left(ye^{-1+y}\right)}{\left(1+\text{LambertW}\left(ye^{-1+y}\right)\right)}\, \frac{1+y}{y}\, \beta(y) \;, \tag{28}$$

a solution is obvious, namely, $\beta(y) \propto \frac{y}{1+y}$. The constant of proportionality is then given by $\ln\lambda = \ln(1/e) = -1$, as in (2), and thus (23) is recovered.

2. Möbius transformation form

This is a simple Padé approximant [12], sometimes known as an "exact" β function [22], and is but a minor variation on the previous two-loop example. For constants α, β, γ, and δ, consider

$$\frac{dg}{dt} = \frac{1}{2}\, g^3\, \frac{\alpha + \beta g^2}{\gamma + \delta g^2} \ . \tag{29}$$

Upon changing variables to

$$y = \frac{\gamma\left(\beta + \alpha/g^2\right)}{\alpha\delta - \beta\gamma} \ , \tag{30}$$

the equation becomes just like (23) with only a change of scale for t:

$$\frac{dy}{dt} = \frac{-\alpha^2}{\alpha\delta - \beta\gamma}\frac{y}{1+y} \ . \tag{31}$$

Thus the solution is

$$y\left(t\right) = \text{LambertW}\left(y_0 e^{y_0 - \frac{\alpha^2}{\alpha\delta-\beta\gamma}t}\right) \ .$$

This is again of FC form with eigenvalue $\lambda = e^{\frac{-\alpha^2}{\alpha\delta-\beta\gamma}}$. In terms of the original variable the RG trajectory is given by

$$g^2\left(t\right) = \frac{-\alpha/\beta}{1 - \left(\frac{\alpha\delta-\beta\gamma}{\beta\gamma}\right)\text{LambertW}\left(\frac{\gamma}{\alpha\delta-\beta\gamma}\left(\beta + \frac{\alpha}{g^2}\right)\exp\left(\frac{\gamma}{\alpha\delta-\beta\gamma}\left(\beta + \frac{\alpha}{g^2}\right) - \frac{1}{\alpha\delta-\beta\gamma}\alpha^2 t\right)\right)} \ . \tag{32}$$

3. One-loop geometromorphosis

This describes the renormalization flow of geometry from a flat manifold in the UV towards a fixed, nontrivial manifold in the IR. The trajectories describe evolution of matrices,

$$\frac{dg_{ab}\left(t\right)}{dt} = \beta_{ab}\left(t\right) \ , \quad g_{ab}\left(t\right) = g_{ab}\left(0\right) + \int_0^t d\tau\ \beta_{ab}\left(\tau\right) \ . \tag{33}$$

For RG flow of this type, we would expect a tensor version of the Schröder equation to be operative,

$$\Psi_{ab}\left(\mathbf{g}\left(1\right)\right) = \Lambda_{ac}\Psi_{cb}\left(\mathbf{g}\left(0\right)\right) \ , \tag{34}$$

where g_{ab} could include the torsion potential as well as the metric (in which case $g_{ab} \neq g_{ba}$) and where the step-scaling function is now a RG transported g_{ab},

$$g_{ab}\left(1\right) = \Lambda_{ac}g_{cb}\left(0\right) \ , \quad \Lambda_{ac} = \delta_{ac} + \left(\int_0^1 d\tau\ \beta_{ad}\left(\tau\right)\right) g^{-1}_{db}\left(0\right) \ . \tag{35}$$

To simplify the discussion, and to be explicit, consider the 3-sphere σ-model with torsion [2], with $\mathfrak{S}$ proportional to the square of the radius of S_3. In this case, the one-loop renormalization of the metric boils down to just a change of $\mathfrak{S}$ with length scale:

$$\frac{d\mathfrak{S}}{dt} = \frac{1}{2}\left(\frac{1}{\mathfrak{S}^2} - 1\right) \ . \tag{36}$$

The solution of this one-loop evolution equation is given implicitly by

$$\frac{\mathfrak{S}(t)+1}{\mathfrak{S}(t)-1}\, e^{-2\mathfrak{S}(t)} = e^t\, \frac{\mathfrak{S}+1}{\mathfrak{S}-1}\, e^{-2\mathfrak{S}} \ . \tag{37}$$

That is to say, (5) and (7) have eigenvalue $\lambda = e$, with explicit Schröder function

$$\Psi(\mathfrak{S}) = \frac{\mathfrak{S}+1}{\mathfrak{S}-1}\, e^{-2\mathfrak{S}} \ , \tag{38}$$

while Ψ^{-1} is only implicit. Note that $\Psi(\mathfrak{S}) > 0$ when $\mathfrak{S} > 1$. The 3-sphere squared-radius RG evolution is then given in FC form by

$$\mathfrak{S}(t) = \Psi^{-1}\left(e^t \Psi(\mathfrak{S})\right) \ , \tag{39}$$

This defines implicitly the step-scaling function $\sigma(\mathfrak{S})$, as $\mathfrak{S}(1)$, say, shown here. The fixed point $\sigma(\mathfrak{S}_*) = \mathfrak{S}_* = 1$ is centered in the small black circle.

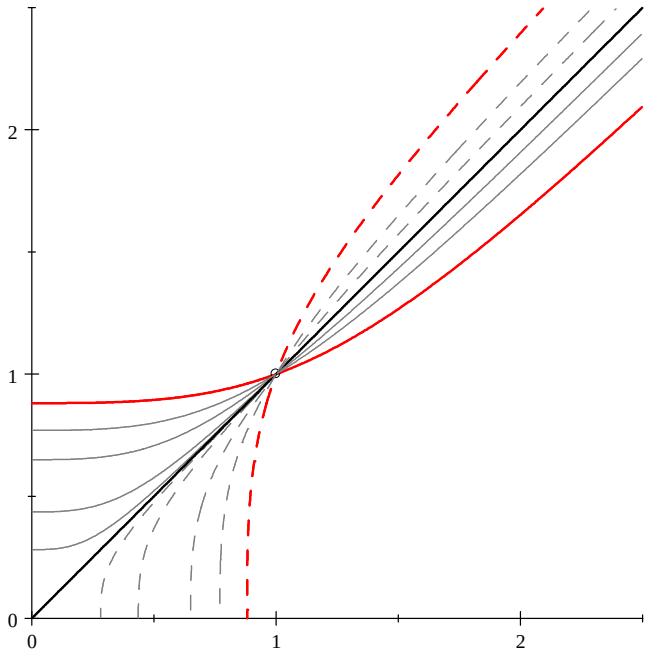

One-loop "geometrostatic" IR fixed point exhibited by $\sigma(\mathfrak{S})$ (solid red) and $\sigma^{-1}(\mathfrak{S})$ (dashed red) versus $\mathfrak{S}$, and a few other fixed t slices of the $\sigma_t(\mathfrak{S})$ surface (thin gray curves).

The implicit function Ψ^{-1} has no name, as far as we can tell, although it might be classified as a generalization of the Lambert function. In any case, we may construct the inverse function $\Psi^{-1}(z)$ through the usual graphical methods, to find two branches.

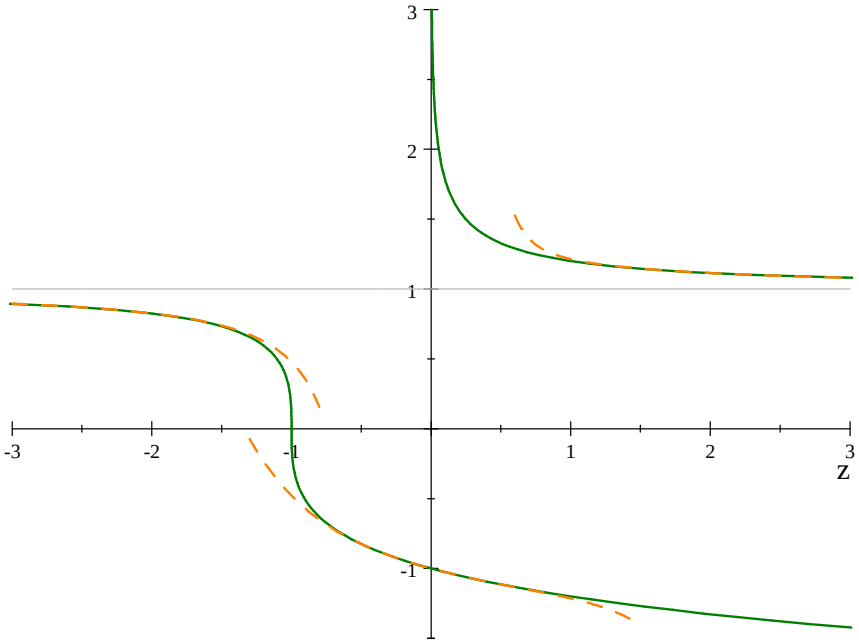

Two branches of $\Psi^{-1}(z)$, in green, and various approximations (orange dashes).

The UV fixed point — a 3-sphere of infinite radius — corresponds to the vertical asymptote of the *upper* branch of Ψ^{-1}, while the IR fixed point — a 3-sphere of unit radius — corresponds to the horizontal asymptote (thin light gray line in the Figure) of that upper branch. Also as shown in the Figure, it is straightforward to construct series approximations around the point $(z, \Psi^{-1}(z)) = (0, -1)$, for the lower branch,

$$\Psi^{-1}_{\text{lower branch}}(z) = -1 - 2e^{-2}z + 6e^{-4}z^2 - 26e^{-6}z^3 + \frac{2}{3}197e^{-8}z^4 - 722e^{-10}z^5 + O\left(z^6\right) \ , \quad (40)$$

as well as around the point(s) $(z, \Psi^{-1}(z)) = (\pm\infty, +1)$, for either the upper or the lower branches,

$$\Psi^{-1}(z) = 1 + 2e^{-2}\left(\frac{1}{z}\right) - 6e^{-4}\left(\frac{1}{z}\right)^2 + 26e^{-6}\left(\frac{1}{z}\right)^3 - \frac{2}{3}197e^{-8}\left(\frac{1}{z}\right)^4 + 722e^{-10}\left(\frac{1}{z}\right)^5 + O\left(\left(\frac{1}{z}\right)^6\right) . \quad (41)$$

The second of these series follows from the first through the transformation $(\Psi, \mathfrak{S}) \to \left(\frac{1}{\Psi}, -\mathfrak{S}\right)$ applied to the equation for Ψ. These series results for Ψ^{-1} are representative

of situations where simple, closed-form expressions are not readily available. A similar situation often arises when we have:

III. A LATTICE GAUGE THEORY MODEL

In this section we consider a physical illustration of fixed point behavior drawn from numerical studies of lattice gauge theory [1]. The β and σ functions in question are those for a non-abelian gauge theory with 12 flavors of $su(3)$ color triplets.

A. Parameterizations

It is convenient in lattice gauge theory to approximate the physical coupling at length scale ℓ, $u = 1/g^2(\ell)$, parametrically in terms of the bare lattice coupling, $s = 1/g_0^2$, as a series [1],

$$u = \frac{1}{g^2(\ell)} = s\left(1 - \sum_{j=1}^{n} c_j(\ell)\frac{1}{s^j}\right) . \tag{42}$$

The step-scaling procedure [4, 20] then gives the coupling at length L as a function of u. Of course, this is also a function of the bare lattice coupling parameter, s, but with a different series expansion, in general, perhaps even with a different order for the series (depending on the choices made in the numerical computations).

$$\sigma(u) = \frac{1}{g^2(L)} = s\left(1 - \sum_{j=1}^{N} c_j(L)\frac{1}{s^j}\right) . \tag{43}$$

Note that these series are arranged to have a common zero-coupling limit, as $s \to \infty$, with both (42) and (43) becoming the identity map in that limit. For this parameterization, the functional equation (18) for $\beta(u)$ may be written as

$$\beta(\sigma(u(s)))\ \frac{du(s)}{ds} = \beta(u(s))\ \frac{d\sigma(u(s))}{ds} , \tag{44}$$

where

$$\frac{du(s)}{ds} = 1 + \sum_{j=1}^{n}(j-1)c_j(\ell)\frac{1}{s^j} \quad \text{and} \quad \frac{d\sigma(u(s))}{ds} = 1 + \sum_{j=1}^{N}(j-1)c_j(L)\frac{1}{s^j} . \tag{45}$$

It is sensible from the stand-point of perturbation theory to consider a similar expansion for β. Thus we write

$$\beta(u) = \sum_{n\geq 0}\frac{b_n}{u^n} . \tag{46}$$

Using this series along with (42), (43), and (45), and expanding both sides of (44) in powers of $1/s$, we obtain recursion relations for the coefficient ratios b_n/b_0. The $O(1)$ and $O(1/s)$ terms on LHS and RHS of (44) match identically, but the $O(1/s^n)$ terms for $n \geq 2$ give expressions for b_{n-1}/b_0 in terms of the $c_{k\leq n}$. For example, we find

$$\frac{b_1}{b_0} = \frac{c_2(L) - c_2(\ell)}{c_1(L) - c_1(\ell)} \ , \quad \frac{b_2}{b_0} = \frac{2c_3(L) - 2c_3(\ell) - (c_1(L) + c_1(\ell))(c_2(L) - c_2(\ell))}{c_1(L) - c_1(\ell)} \ , \tag{47}$$

etc. The overall normalization of β is not determined by (44), of course, and in fact there is no information in the expansions (42), (43), and (45) that allows determination of b_0 by Taylor expanding about $s = \infty$. (This is related to the essential singularity in the Schröder function solutions at zero coupling, as mentioned earlier, (15) et seq.) Rather, we must fix b_0 by other considerations, the obvious choice being to use perturbation theory. Another possibility is to use lattice data and expand, not about zero coupling, but about a nontrivial fixed point, if available. The expansions are similar to those we have just given, and are collected together in the Appendix, §IX.

B. Numerics

Considerable effort is needed to properly take the continuum limit where the lattice spacing a goes to zero. However, for purposes of *illustration* of the various functional methods described here, we will not concern ourselves with those complications. Rather, we will simply take some of the raw numerical data in [1] for the expansion coefficients appearing in (42) and (43), and note with amusement that such a naive *ab initio* computation of the β function matches very well with two-loop perturbation theory, upon overlapping the two results.

We choose to consider the $L = 8a$ and $L = 16a$ data from [1] for 12 flavors of $su(3)$ color triplets, a model widely believed to have a nontrivial IR fixed point near $g^2 = 5$. We take the data at face value, without regard for any statistical or systematic errors, and we use this data for the parametric definitions of u and $\sigma(u)$.

$$u(s) = s\left(1 - 0.4092\left(\frac{1}{s}\right) + 0.192\left(\frac{1}{s}\right)^2 - 0.73\left(\frac{1}{s}\right)^3 + 0.837\left(\frac{1}{s}\right)^4 - 0.342\left(\frac{1}{s}\right)^5\right) \ ,$$

$$\sigma(u(s)) = s\left(1 - 0.467\left(\frac{1}{s}\right) + 0.154\left(\frac{1}{s}\right)^2 - 0.164\left(\frac{1}{s}\right)^3\right) \ . \tag{48}$$

For illustration purposes, this will suffice; but, hopefully, the procedures we follow will be useful in future, realistic lattice studies.

In any case, we plot $\sigma(u)$, parametrically, versus u to display the $\sigma(u_*) = u_* = 1/g_*^2$ fixed point encoded in the data, as given numerically by:

$$g_*^2 = \frac{1}{0.180} = 5.56 \quad \text{at} \quad s = 0.739 \ , \quad \text{i.e.} \quad g_{0*}^2 = \frac{1}{0.739} = 1.35 \ . \tag{49}$$

The two series (48) were *constructed* to become parallel curves in the zero coupling limit, as s or $u \to \infty$. However, the curves have significantly different approaches to the nontrivial fixed point, hence its existence, as is evident in the Figure. The fixed point $u_* = 0.180$ is centered in the small black circle.

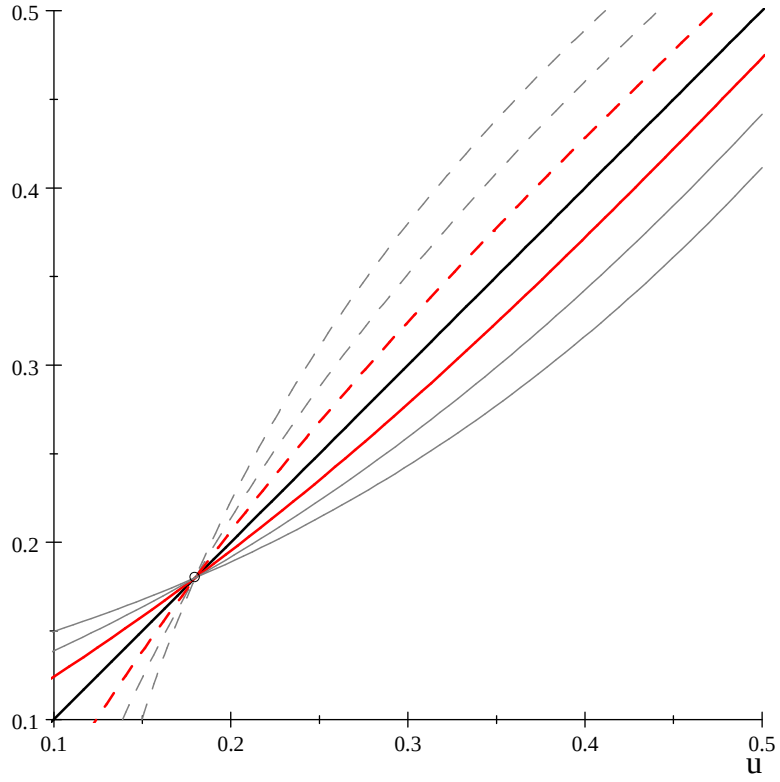

$\sigma(u)$ (solid red) and $\sigma^{-1}(u)$ (dashed red) versus u, and a few other fixed t slices of the $\sigma_t(u)$ surface (thin gray curves).

Now, if we use the s-parameterization formalism discussed above, we obtain for example:

$$\frac{b_1}{b_0} = 0.657 \ , \quad \frac{b_2}{b_0} = -20.2 \ . \tag{50}$$

This certainly *looks* useless (i.e. like a divergent series for $g^2 \gtrapprox 0.03$) and is very much in

disagreement with perturbation theory, as given to 2-loops for the 12 flavor $su(3)$ model by

$$\frac{d}{dt}u = -2\left(\frac{3}{(4\pi)^2} - \frac{50}{(4\pi)^4}\frac{1}{u}\right) \ , \tag{51}$$

such that $b_1/b_0 = -\frac{50}{3(4\pi)^2} = -0.106$. But if nothing else, (50) confirms that the data in (48) certainly did not come just from transcribing perturbation theory.

On the other hand, if we reparameterize the data around the IR fixed point, defining

$$\frac{1}{s} = (1+r)\, g_{0*}^2 \ , \tag{52}$$

and expand various quantitites to and including $O(r^4)$, as described in detail in an Appendix, we find

$$\begin{aligned} u(r) &= 0.180 - 1.52r - 1.258r^2 - 3.25r^3 - 0.408r^4 - 0.739r^5 + O\left(r^6\right) \ , \\ \sigma(u(r)) &= 0.180 - 1.13r + 0.439r^2 - 0.739r^3 + 0.739r^4 + O\left(r^5\right) \ . \end{aligned} \tag{53}$$

Admittedly, the second of these r-series is less firm, since we only have $\sigma(u(s))$ to $O\left(\left(\frac{1}{s}\right)^3\right)$, although the difference will turn out to be slight over the region where the series is reliable. We describe below the changes encountered from truncating the $\sigma(u(r))$ series at $O(r^3)$ versus $O(r^4)$.

Using again the functional formalism to determine the β function from σ, only now as implemented in terms of the expansion about the nontrivial fixed point (for details, see the Appendix), we find the more sensible expression

$$\beta(u) = \beta(u_* + w) = \mathfrak{b}_1 \times \left(w - 3.14w^2 + 1.86w^3 + 4.02w^4\right) \ , \quad \text{where} \quad \mathfrak{b}_1 = \ln(0.745) = -0.294 \ . \tag{54}$$

This is the best one can do given only the data in (48). So, small, positive initial w will decrease as t increases. That is to say, $u > u_*$ will decrease down to u_* as t increases. Or, since $u = 1/g^2$, $g^2 < g_*^2$ will increase up to g_*^2 as t increases. Increasing t corresponds to increasing length scale, so the fixed point is indeed an IR one. This is clear from computing the trajectories that follow from (54). Here is an example of $g^2(t)$, with $g^2(0) = 3$.

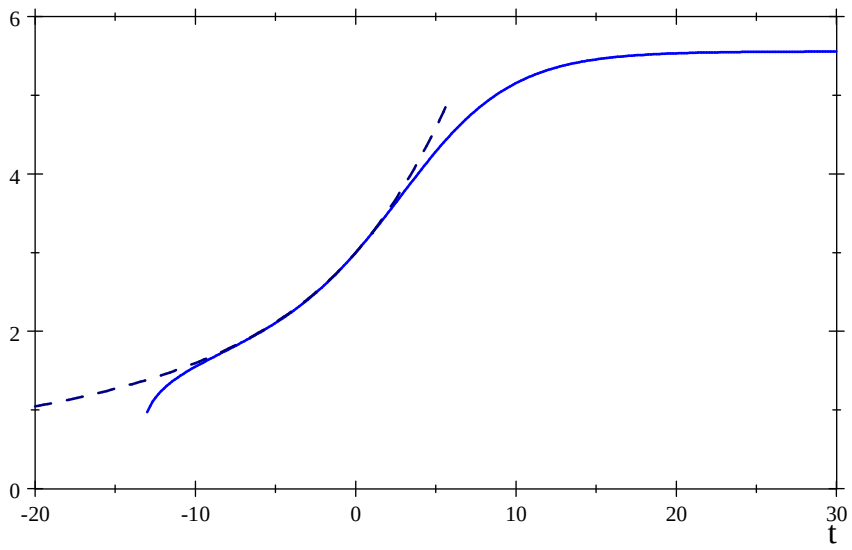

Lattice (solid blue) and 2-loop (dashed blue) $g^2(t)$ trajectories, with $g^2(0) = 3$.

In terms of both slope and curvature (cf. cubic splines), the trajectory joins very smoothly with that obtained from two-loop perturbation theory for 12 flavors of quark color triplets.

Further comparison can be made to trajectories determined by other approximations. It is more direct, however, to just compare β functions, now that we have in hand (54). In addition to the two-loop approximation, which is unchanged by analytic redefinitions of the coupling, we also compare to three-loop (minimally subtracted, as well as that based on the Schrödinger — not Schröder — functional) and to four-loop results from perturbation theory (see [1] for the literature dealing with these approximations). Note how well the two-loop result joins smoothly to our naive, but ab initio determination of β using the lattice data and functional methods, at $g^2 = 3$. We stress that there have been *no* adjustments in the normalizations to facilitate this match-up. The other, higher-loop approximations do not fare nearly as well in terms of matching-up with the lattice β, although they do give estimates of g_*^2 more or less in line with (49).

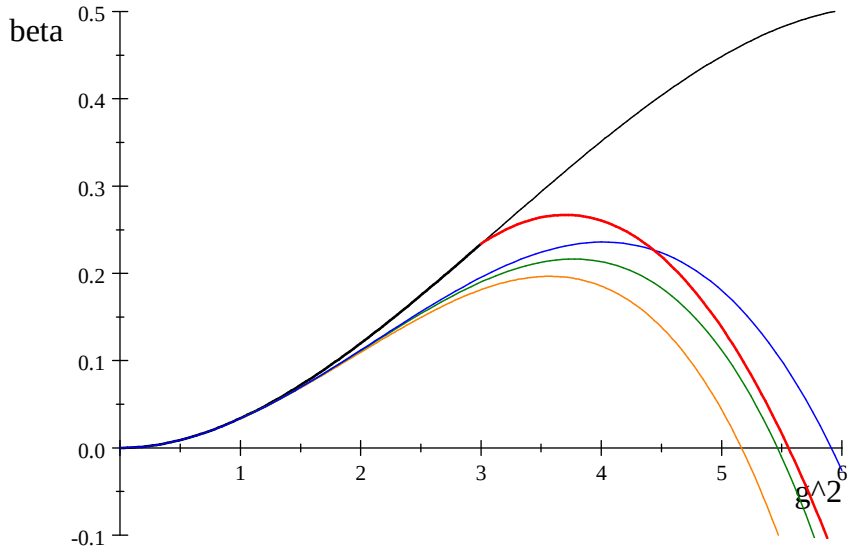

Various $\beta\left(g^2\right)$ functions: 2-loop (black), 3-loop MS (green), 3-loop SFR (orange), 4-loop MS (blue), lattice (red).

Finally, we contrast the differences resulting from truncating the $\sigma\left(u\left(r\right)\right)$ series at $O\left(r^3\right)$ versus $O\left(r^4\right)$. The resulting changes in $\beta\left(g^2\right)$, as obtained from the step-scaling function, are shown below. The difference is slight near $g^2 = 3$, but becomes a sizeable disagreement for $g^2 \lessapprox 2.5$, at which point the disparity is comparable to that between (54) and the higher-loop approximations at $g^2 = 3$. In fact, the $O\left(r^3\right)$ truncation even gives another, spurious(!) nontrivial fixed point at $g^2 \approx 1.7$. Simply put, for $g^2 \lessapprox 2.5$ the $O\left(w^4\right)$ series in (54) is woefully inadequate. A better approximation to the solution of the β functional equation must be used for smaller g^2.

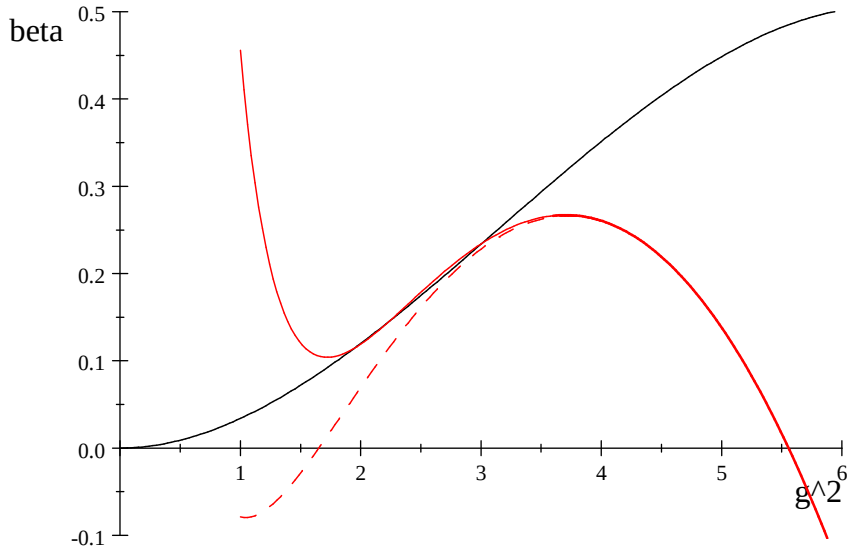

Two-loop (black) and lattice (red) βs, the latter to both cubic (dashed) and quartic order.

While some of these numerical coincidences may very well be little more than artefacts of the data selected, it is of interest to see if this match-up between perturbative results, and those obtained for β by functional methods, persists given more accurate lattice data and a thorough analysis of numerical errors. The above discussion is an illustrative application of the functional methods introduced here, rather than an endorsement of specific results.

IV. A MODEL WITH A LIMIT CYCLE

In this section we illustrate elementary limit cycle behavior in an exactly solvable lattice model, albeit one-dimensional, as obtained in [17] by an extension of the standard BCS Hamiltonian to include a term that breaks time-reversal invariance. A model with similar RG structure was studied in [15]. As before, we emphasize the connections between discrete and continuous scaling, and the underlying functional relationships.

The physics of the model is explained in the extensive work of LeClair et al. and only the key mathematical features will only be summarized here. The Hamiltonian for the model is

$$H = \sum_j \varepsilon_j b_j^\dagger b_j + \sum_{j,k} V_{jk} b_j^\dagger b_k \ , \qquad V_{jk} = \begin{cases} (g+ih)\,\epsilon & \text{if } \varepsilon_j > \varepsilon_k \\ g\epsilon & \text{if } \varepsilon_j = \varepsilon_k \\ (g-ih)\,\epsilon & \text{if } \varepsilon_j < \varepsilon_k \end{cases} , \tag{55}$$

where b_j and $b_j^\dagger$ denote the usual Cooper-pair annihilation and creation operators, and where $\epsilon = \frac{1}{2}\left(\varepsilon_{j+1} - \varepsilon_j\right)$ is the single-particle level spacing.

For a large number of system sites, the renormalization of the dimensionless couplings g and h under a change in system size L is given by

$$\frac{dg}{d\ln L} = g^2 + h^2 \ , \quad h = \text{constant} \ , \tag{56}$$

with h the time-reversal breaking parameter. Assuming $h \neq 0$, we change variables to $u = g/h$ and $t = h \ln L$. Then

$$\frac{du}{dt} = 1 + u^2 \ , \tag{57}$$

and direct integration gives

$$u\,(t) = \tan\left(t + \arctan u_0\right) \ . \tag{58}$$

Thus the physics of the model repeats itself cyclically as the logarithm of the system size is changed.

On the other hand, the functional conjugacy formalism gives

$$\Psi(u) = \exp\left(\int^u \frac{dw}{1+w^2}\right) = \exp(\arctan u) \ , \quad \Psi^{-1}(u) = \tan(\ln u) \tag{59}$$

$$u(t) = \Psi^{-1}\left(\lambda^t \Psi(u_0)\right) = \tan(t \ln \lambda + \arctan u_0) \tag{60}$$

Comparing the last expression to (58) we see that the Schröder eigenvalue for a unit step in t is $\lambda = e$.

In general, the step-scaling function corresponding to t step size Δ is

$$\sigma(u) \equiv u(t)|_{t=\Delta} = \tan(\Delta + \arctan u) = \frac{u + \tan\Delta}{1 - u\tan\Delta} \ . \tag{61}$$

Choosing $\Delta = \pi/4$ for convenience, a quick check on (18) gives

$$\beta(u) = 1 + u^2 \ , \quad \sigma(u) = \frac{1+u}{1-u} \ , \quad \frac{d\sigma(u)}{du} = \frac{2}{(1-u)^2} \ , \tag{62}$$

So $\beta(\sigma(u)) = \frac{d\sigma(u)}{du}\ \beta(u)$ indeed holds. In fact, the functional equation obeyed by Ψ, namely,

$$e^{\Delta}\ \Psi(u) = \Psi\left(\frac{u + \tan\Delta}{1 - u\tan\Delta}\right) \ , \tag{63}$$

actually belongs to the first class of examples discussed in §2 of the original paper by Schröder [23]. (As an aside, we also note that (57) is a complexified form of the Beverton–Holt–Skellam model from population dynamics [10].)

The trajectory (60) describes a limit cycle because it is periodic in t, as observed by LeClair et al. [17] (also see [15]). This is clearly a consequence of Ψ^{-1} being periodic, as we remarked earlier in a general context, in §II. However, the discontinuity in the trajectory is somewhat peculiar to the model. This discontinuity is also displayed by the step scaling function, as shown in the Figure.

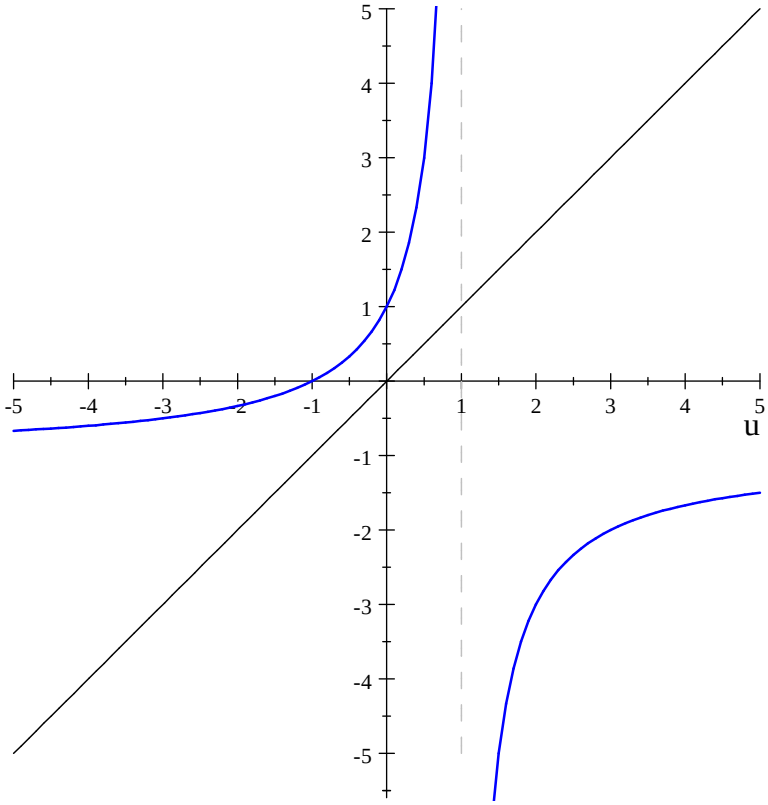

Step-scaling function $\sigma(u) = \tan\left(\frac{\pi}{4} + \arctan u\right)$, in blue, compared to the identity map. Note the discontinuity at $u = 1$ and the lack of a real fixed point.

Since σ does *not* intercept the identity map there is no *real* fixed point in this case, although Ψ can be constructed by series solution about the purely imaginary fixed points at $u = \pm i$.

We defer to the detailed discussions in [17] for a more complete picture of the physics described by this example. We return to a model-independent viewpoint, to explore other ways that limit cycles might be encountered.

V. MORE ON THE β FUNCTIONAL EQUATION

For emphasis, we state again the functional equation relating the renormalization "velocity" β to the step-scaling function σ.

$$\beta(\sigma(u)) = \frac{d\sigma(u)}{du}\,\beta(u) \quad . \tag{18}$$

Generally speaking, if β is known, this (nonlinear) functional equation determines $\sigma(u)$, up to a constant of integration, while if $\sigma(u)$ is known, the equation determines β, again up to a (normalization) constant. However, the equation may hold in store some surprises.

A fixed point u_* in the step-scaling scheme *must* obey $\sigma(u_*) = u_*$. Thus at a fixed point, it is trivially true that $\beta(\sigma(u_*)) = \beta(u_*)$. But what has this to do with the standard fixed point condition that $\beta(u_*) = 0$? If $d\sigma/du|_{u_*} \neq 1$, then it would *seem* to follow from the functional equation that $\beta(u_*) = 0$ when $\sigma(u_*) = u_*$, while if $d\sigma/du|_{u_*} = 1$, the functional equation itself would not lead to any conclusion about the value of $\beta(u_*)$. But there is a subtle assumption here: All this is true if there is only *one branch* of the analytic function giving rise to β. Related to this, a *zero* in $d\sigma/du$ may induce, coincide with, or even supplant a zero of β. This is at odds with the *usual* renormalization group point of view, but in general this too can occur, and when it does, it may foreshadow a much richer renormalization structure.

If we have a zero in $d\sigma/du$, say at u_0, and $\beta(u_0)$ is finite, then the functional equation implies $\beta(\sigma(u_0)) = 0$. Now, in the *usual* renormalization group situation, which we may describe as a purely *first-order* framework, $u(t)$ is completely determined by $u(t_0)$ and a single function $\beta(u) = du/dt$. So, if $\beta(\sigma(u_0)) = 0$ and $\sigma(u)$ is just the initial u after having been t-evolved for some discrete step in t, this means that $\sigma(u_0) = u_0$, and therefore $\beta(u_0) = 0$ must also hold. The fact that $d\sigma/du|_{u_0}$vanishes does not make much difference in this purely first-order point of view [31].

However, in the *quasi-Hamiltonian* framework defined and discussed in [8], it may be that $\sigma(u_0)$ is not just a zero of β, but rather it is a *branch point* of an analytic function whose various branches constitute a *family* of βs. In this situation, to completely determine the t-evolution of u it is necessary to specify a transition function. That is to say, it is necessary to give a prescription describing how the trajectory switches from one branch of β to another when the branch point $\sigma(u_0)$ is encountered.

In this approach, $\sigma(u_0)$ is a "turning point" in the evolution, and not necessarily a fixed point. Hence it is not necessary for $\sigma(u_0)$ to be the same as u_0. Nor is it necessary for $\beta(u_0)$ to vanish.

The quasi-Hamiltonian approach brings to mind a Hamiltonian system whose underlying dynamics is actually a second-order differential equation, but which has been reduced to a first-order system between turning points through the use of energy conservation (see the first Appendix). Thus one would expect, at the very least, that the corresponding β function could flip sign at the turning point $\sigma(u_0)$.

In fact, the situation can be more complicated. There may be *more* than the two branch

choices $\pm|\beta|$ at the turning point. In general there may be an *infinite* number of branches from which to choose β!

A local, differential way to think about the various alternatives is to consider the RG *acceleration*, *jerk*, etc., along the trajectory as computed through use of the chain rule:

$$\frac{d^n\beta(u)}{dt^n} = \beta(u)\ \frac{d}{du}\left(\frac{d^{n-1}\beta(u)}{dt^{n-1}}\right)\ . \tag{64}$$

So, for instance, if

$$\beta(u) \underset{u\to\sigma(u_0)}{\sim} (\sigma(u_0)-u)^p\ , \tag{65}$$

then

$$\frac{d^n\beta(u)}{dt^n} \underset{u\to\sigma(u_0)}{\sim} (\sigma(u_0)-u)^{(n+1)p-n}\ . \tag{66}$$

Thus, even though $\beta(\sigma(u_0))=0$, the RG acceleration $d\beta/dt$ can be nonzero at $u=\sigma(u_0)$ if $0<p\leq 1/2$, indicating that $\sigma(u_0)$ is a turning point and not a fixed point for the continuous flow under these circumstances.

All these things are best understood through consideration of some toy models.

VI. TOY MODELS AND NOVEL BEHAVIOR

Consider a toy example that is unphysical (so far as we are aware) but can be solved in closed form [23],

$$\sigma(u) = 2u(1-u) \ . \tag{67}$$

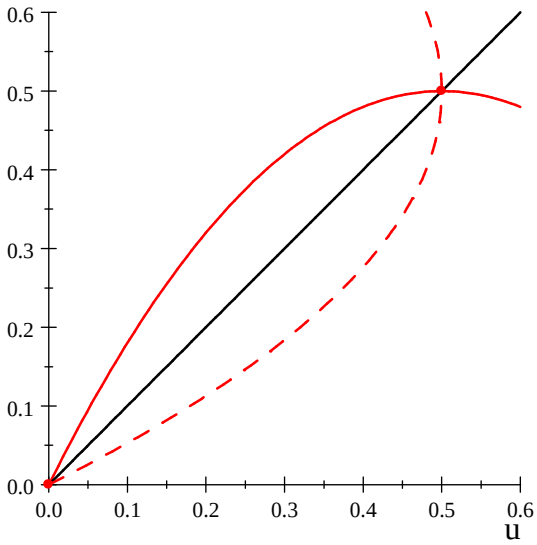

Toy model $\sigma(u) = 2u(1-u)$ (solid red) and $\sigma^{-1}(u)$ (dashed red) versus u.

There are fixed points of $\sigma(u)$ at 0 and $u_* = 1/2$, as indicated by red dots in the Figure. The functional equation for the β function in this case is

$$\beta(2u(1-u)) = 2(1-2u)\beta(u) \ , \tag{68}$$

with the normalization determined to be $\ln 2$ from the eigenvalue of Schröder's equation at $u = 0$, namely, $2\Psi(u) = \Psi(2u(1-u))$. Series solution of the functional equation for β about $u = 0$ immediately gives

$$\beta(u)/\ln 2 = u - u^2 - \frac{2}{3}u^3 - \frac{2}{3}u^4 - \frac{4}{5}u^5 - \frac{16}{15}u^6 - \frac{32}{21}u^7 + \cdots = \frac{1}{2}(2u-1)\ln(1-2u) \ , \tag{69}$$

where the latter closed form is not difficult to guess from the first twenty or so terms in the explicit series, and is easily checked to solve the functional equation exactly. This β has zeroes precisely at the fixed points of σ, again as indicated by red dots in the following Figure.

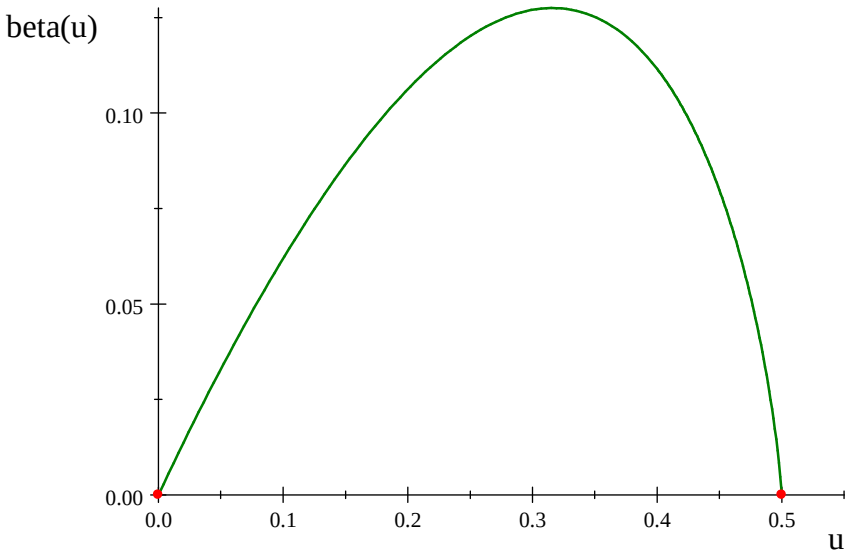

The toy β function, $\beta(u) = \frac{1}{2}(\ln 2)(2u-1)\ln(1-2u)$.

For this special case, $d\sigma/du = 2(1-2u)$ vanishes at $u_* = 1/2$, the nontrivial fixed point of σ, and in addition $\beta(1/2) = 0$, but these coincidences are *not* true in general, as we shall see. In fact, in spite of the divergence in $d\beta(u)/du|_{u=u_*}$, both the RG acceleration and the RG jerk vanish at the nontrivial fixed point, $\frac{d}{dt}\beta(u_*) = 0 = \frac{d^2}{dt^2}\beta(u_*)$, as do all higher t derivatives of β, since $\lim_{u\to 1/2}(2u-1)\ln^n(1-2u) = 0$ for any n. Thus in this case the RG flow into the nontrivial fixed point takes place with a very "soft landing."

Integration of $du/dt = \beta(u)$ gives

$$u(t) = \frac{1}{2}\left(1 - (1-2u(0))^{2^t}\right) \ . \tag{70}$$

This is precisely of the FC form sanctioned by Schröder, namely, $u(t) = \Psi^{-1}(2^t\Psi(u(0)))$, with $\Psi(x) = \ln(1-2x)$ and $\Psi^{-1}(x) = \frac{1}{2}(1-e^x)$. A representative trajectory is shown here.

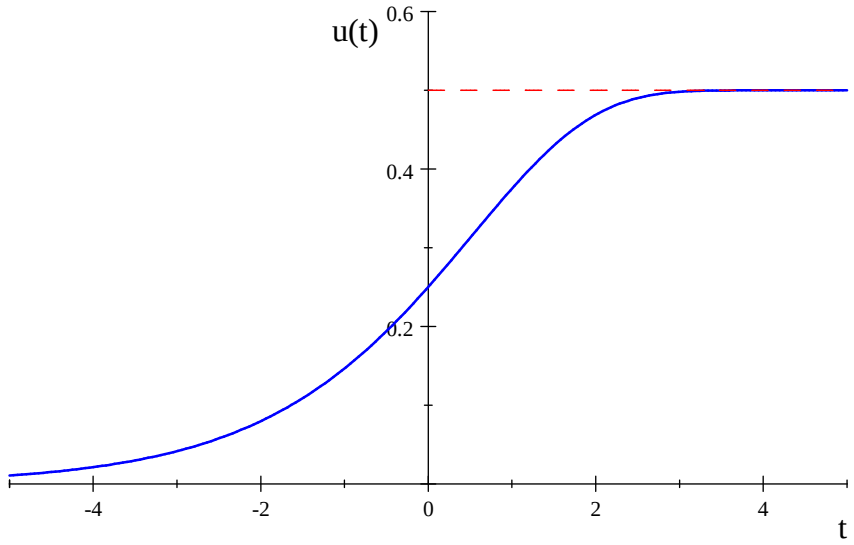

A trajectory for the $\sigma(u) = 2u(1-u)$ model, with $u(0) = 1/4$.

More generally, consider toy models for step-scaling functions based on the logistic map [6, 11]. For parameter s, with $0 \leq s \leq 4$, let

$$\sigma(u, s) = s\ u(1-u) \ . \tag{71}$$

This σ has fixed points at 0 and $u_* = 1 - \frac{1}{s}$. Except for the special case $s = 2$, u_* does *not* coincide with the location of the maximum of the map where $d\sigma/du = 0$, as given by $\sigma(1/2) = s/4$.

The functional equation for the β function in this case is

$$\beta(su(1-u), s) = s(1-2u)\beta(u, s) \ , \tag{72}$$

where the normalization of the solution is given by $\ln(s)$. That is to say, $\beta = (\ln s)\ \Psi/(d\Psi/du)$ where Ψ is the corresponding solution of Schröder's equation with eigenvalue s.

$$s\ \Psi(u, s) = \Psi(s\ u(1-u), s) \ . \tag{73}$$

While these functional equations do not admit closed-form solutions, for generic s, they can be solved numerically with sufficient accuracy for our purposes here through a combination of series and functional methods.

One striking result of this numerical analysis is that $\beta(u_*) \neq 0$, for $2 < s \leq 4$, so the fixed point of the step-scaling function is actually *not* a true fixed point under continuous changes in scale!

Explicit series solution of the functional equation for β about $u = 0$ gives

$$\beta(u,s)/(\ln s) = u - \frac{1}{s-1}\,u^2 - \frac{2}{s^2-1}\,u^3 - \frac{4+5s}{(s^2-1)(s^2+s+1)}\,u^4$$
$$-2\frac{4+5s+7s^2}{(s^2-1)(s^2+s+1)(s^2+1)}\,u^5 - 2\frac{8+18s+31s^2+42s^3+35s^4+21s^5}{(s^2-1)(s^2+1)(s^4+s^3+s^2+s+1)(s^2+s+1)}\,u^6$$
$$-4\frac{8+10s+21s^2+25s^3+39s^4+21s^5+33s^6}{(s^2-1)(s^2+1)(s^4+s^3+s^2+s+1)(s^2+s+1)(s^2-s+1)}\,u^7 + O\left(u^8\right)\ . \qquad (74)$$

More generally we write

$$\beta(u,s)/(\ln s) = u\left(1 + \sum_{n=1}^{\infty} c_n(s)\ u^n\right)\ , \quad c_1 = \frac{1}{1-s}\ , \quad c_2 = \frac{2}{1-s^2}\ , \qquad (75)$$

with higher coefficients in the series given by the recursion relation (here $\lfloor\cdots\rfloor$ is the integer-valued floor function)

$$c_{n+2}(s) = \frac{1}{1-s^{n+2}}\left(2c_{n+1}(s) + \sum_{j=\left\lfloor\frac{n+1}{2}\right\rfloor}^{n+1}\binom{j+1}{2j-1-n}(-1)^{n-j}\,s^j c_j(s)\right) \quad \text{for } n \geq 1. \qquad (76)$$

Numerical study [9] of $c_n(s)$, for various values of s and $n \leq 200$, provides compelling evidence that (75) converges for $|u| < R(s)$ where

$$R(s) = \frac{1}{\limsup\limits_{n\to\infty}\left(|c_n(s)|^{1/n}\right)} = \begin{cases} \dfrac{1}{2} & \text{if } 0 < s \leq \frac{2}{3}\ , \\ \left|1 - \dfrac{1}{s}\right| & \text{if } \frac{2}{3} \leq s \leq 2\ , \\ \dfrac{s}{4} & \text{if } 2 \leq s \leq 4\ . \end{cases} \qquad (77)$$

A closed form is not known for (75), except for $s = 0$, ± 2, and 4. Nonetheless, as already mentioned, the model is amenable to numerical analysis for generic s.

In particular, the functional equation can be exploited to continue the series and exhibit the various branches, β_n, of the multi-valued β function that is encountered for $2 < s \leq 4$ [9]. For example,

$$\beta_0(u,s) = \sqrt{s^2-4su}\ \beta\left(\frac{1}{2s}\left(s - \sqrt{s^2-4su}\right), s\right)\ , \qquad (78a)$$

$$\beta_1(u,s) = -\sqrt{s^2-4su}\ \beta_0\left(\frac{1}{2s}\left(s + \sqrt{s^2-4su}\right), s\right)\ , \qquad (78b)$$

where β is the explicit series (75), β_0 is the continuation of this series through use of the functional equation to give the principal branch on the interval, $0 \leq u \leq s/4$, and β_1 is the first alternative branch which is real-valued on the sub-interval $\frac{1}{4}s^2\left(1-\frac{1}{4}s\right) \leq u \leq \frac{s}{4}$. Etc. For $s \leq 2$ only one branch is needed, namely, β_0, but additional branches, such as β_1, are required to develop completely the trajectories for $s > 2$. In the latter situation, an infinite sequence of real-valued branch functions is given by iterating the definition of β_1. Thus,

$$\beta_{n+1}(u,s) = -\sqrt{s^2-4su}\;\beta_n\left(\frac{1}{2s}\left(s+\sqrt{s^2-4su}\right),s\right)\;. \tag{79}$$

These are all the additional branches of β that are needed for $2 < s \leq 3$ and for $s = 4$, but for $3 < s < 4$ there are other branch function sequences that must be taken into account to describe fully the continuous trajectory $u(t)$.

By construction, stemming from the fact that σ is quadratic, for $s > 2$ the branches of β given by (79) have *square-root zeroes* at points obtained by iterating the action of the step-scaling function, starting from $u_0 = 1/2$. That is, zeroes are given by the sequence $\{\sigma(u_0), \sigma(\sigma(u_0)), \cdots\}$. Thus the β_n branches arrive at those zeroes with infinite slope, exactly as described by (65), and its u derivative, with $p = 1/2$. On the other hand, the product $\beta\; d\beta/du = d\beta/dt$ is finite and nonvanishing in the limit as u goes to one of these zeroes. Consequently, the RG acceleration does not vanish for points in the sequence of β zeroes: They are turning points, not fixed points.

Further general discussion of this class of toy models would take us too far afield. Suffice it to consider here three other explicit examples, two based on numerical analysis ($s = 11/4$ and $s = 10/3$), and one based on elementary closed-form expressions ($s = 4$). For convenience, we first take $s = 11/4$. This gives a step-scaling model $\sigma(u) = \frac{11}{4}\;u(1-u)$, with fixed points at 0 and $u_* = 7/11$.

Constructing graphs like those for the previous toy model, we find that there are several interesting differences between the Figures for the two models. The slope of the step-scaling function is now negative at the nontrivial fixed point, as opposed to the vanishing slope of the previous toy model. This negative slope is a crucial ingredient that gives rise to the multi-valued-ness of the β function, as shown in the Figures.

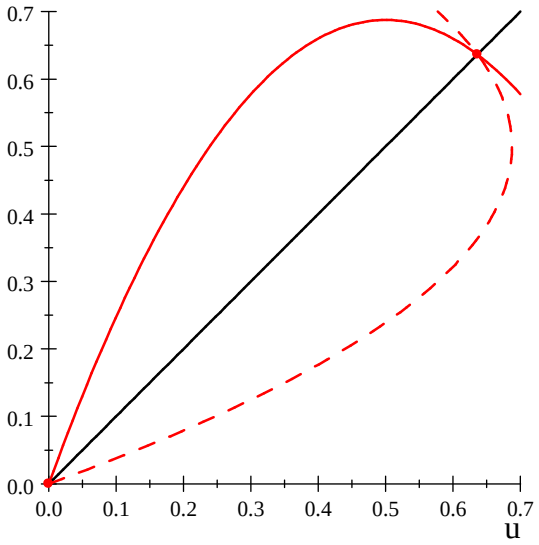

Toy model $\sigma(u) = \frac{11}{4}\, u\,(1-u)$ (solid red) and $\sigma^{-1}(u)$ (dashed red) versus u.

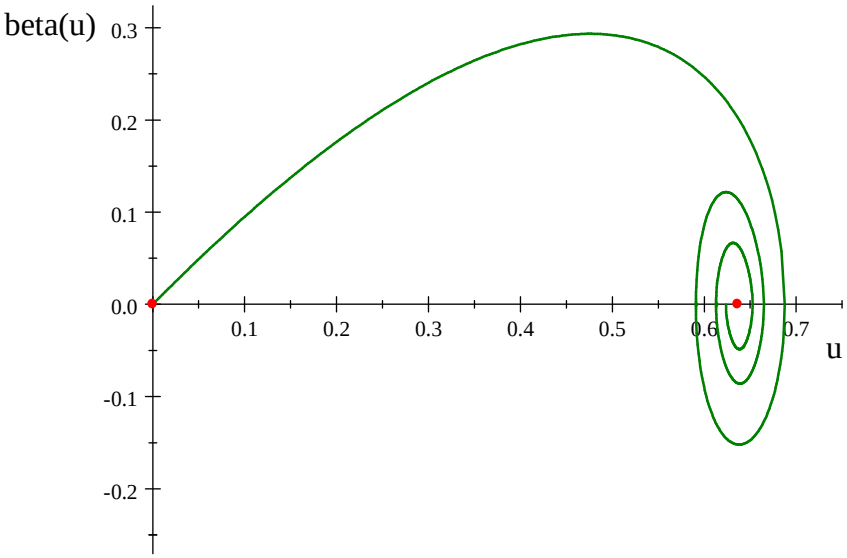

Six branches of the multi-valued β function for the model with $\sigma(u) = \frac{11}{4}\, u\,(1-u)$.

To avoid confusion, we emphasize that this last "phase-space" Figure shows the real-valued branches of $\beta(u)$, i.e. the Figure does **not** show a trajectory in a two-dimensional coupling space. The trajectory $u(t)$ is *one*-dimensional, just as it was in the previous toy model, as illustrated in the following graph. Although $u_* = 7/11$ is a fixed point of σ, it is *not* a zero of β on *any* of its real-valued branches. Moreover, at the nontrivial zeroes of β the RG acceleration does not vanish because the relevant branch of β has a compensating infinite slope, as discussed more generally following (79), and as is evident in the plot of the

toy trajectory, so these zeroes are indeed turning points. Nevertheless, the net effect of the multiple branches of β on the trajectory $u(t)$ is to produce an oscillatory convergence to $u_* = 7/11$ as $t \to \infty$. This is distinctly different from the monotonic approach to $u_* = 1/2$ of the previous toy model whose β function had only one real branch.

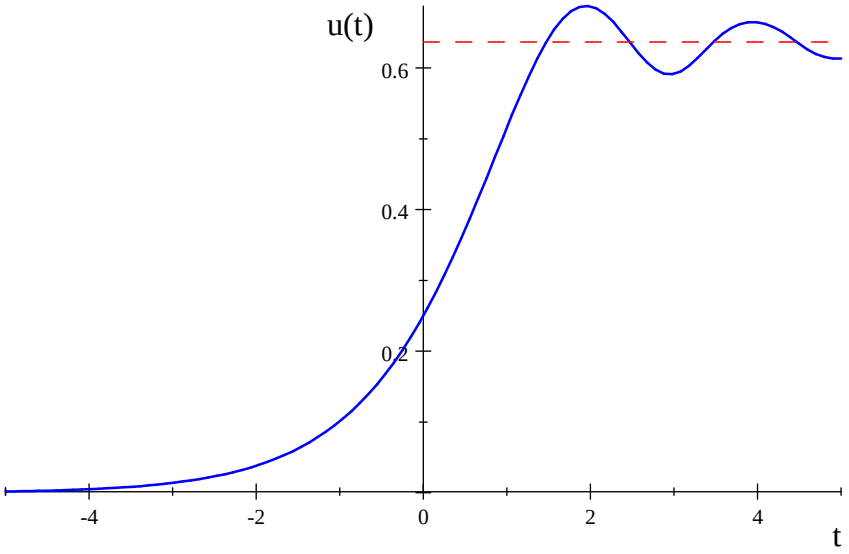

A trajectory with $u(0) = 1/4$, for the $s = 11/4$ multi-valued β function.

Next, consider $s = 10/3$, another case which yields to numerical analysis but cannot be described with closed-form results. The step-scaling function in this case is $\sigma(u) = \frac{10}{3}\, u(1-u)$, with fixed points at 0 and $u_* = 7/10$. The graph of σ is similar to the previous $s = 11/4$ example, and is left to the reader to plot. This toy example is especially interesting in that it provides an explicit RG realization of a *limit cycle*, a possibility conjectured by Wilson in his early, classic study [26], but not thought to be possible for a model with only one coupling until relatively recently [27]. Here, the exact cycle is only realized *asymptotically* in the limit of very large t.

The basic mechanism whereby this is achieved for the $s = 10/3$ case is the same as in the previous toy model: There are an infinite number of branches of the underlying analytic β function, and the evolving RG trajectory switches from one branch to another when turning points are encountered. The branch structure is more complicated for $s = 10/3$ than for $s = 11/4$, however, with the branch points accumulating around $u_{\rm low} = \frac{13}{20} - \frac{1}{20}\sqrt{13} = 0.4697$ and $u_{\rm high} = \frac{1}{20}\sqrt{13} + \frac{13}{20} = 0.8303$ in such a way that, as $t \to \infty$, the trajectory approaches a rectangular sequence of steps between these two values, hence giving rise to a two-cycle asymptotically in t. The initial stages of this large t behavior are evident in the following

sample trajectory.

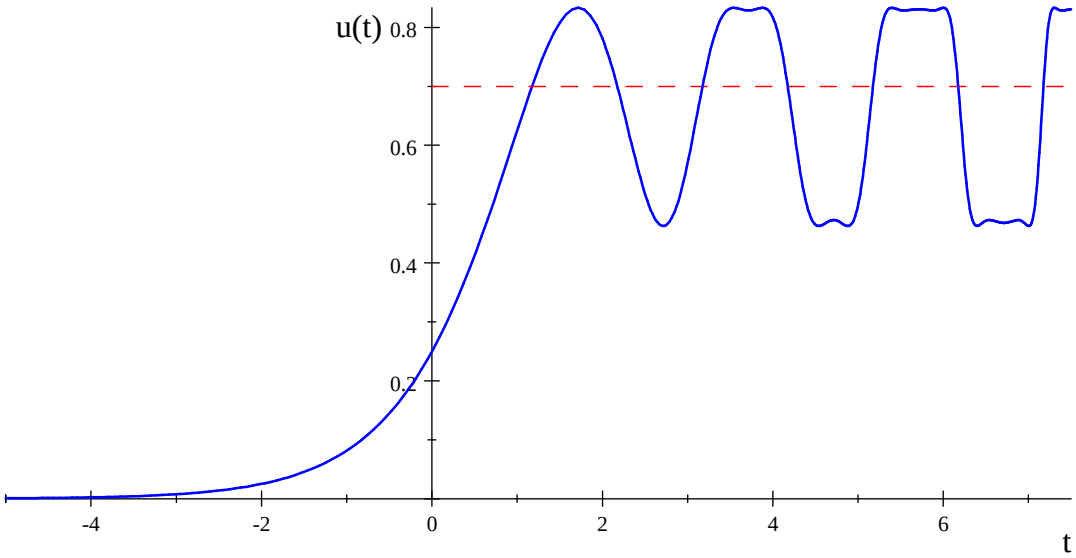

A trajectory with $u\,(0) = 1/4$, for the $s = 10/3$ multi-valued β function with a 2-cycle limit.

While the methods used in the previous example are also applicable to this case (see (78a), (78b), (79), and generalizations), we will not construct here the actual branches of β for $s = 10/3$, nor will we enumerate the sequencing of the various branches as the trajectory evolves. This information can be found, in a different context, in [9]. Suffice it to say that although $u_* = 7/10$ is a fixed point of σ, once again it is *not* a zero of β on *any* of its real-valued branches.

For a final, *chaotic* example, which nevertheless admits an exact, closed-form solution [23], consider

$$\sigma\,(u) = 4u\,(1-u)\ , \tag{80}$$

for $0 \le u \le 1$. In this case the real-valued branches of the analytic β function are given by

$$\beta_n\,(u) = (\ln 4)\,\sqrt{u\,(1-u)}\left((-1)^n\left\lfloor\frac{1+n}{2}\right\rfloor\pi + \arcsin\sqrt{u}\right)\ , \tag{81}$$

for all integer $n \ge 0$. The functional equation is indeed obeyed, in the following sense:

$$\beta_n\,(\sigma\,(u)) = \beta_n\,(u)\ \ d\sigma\,(u)\,/du \quad \text{for} \quad 0 \le u \le 1/2\ , \tag{82a}$$

$$\beta_{n+1}\,(\sigma\,(u)) = \beta_n\,(u)\ \ d\sigma\,(u)\,/du \quad \text{for} \quad 1/2 \le u \le 1\ . \tag{82b}$$

Note that $\sigma\,(u)$ approaches the branch point at $\sigma = 1$ as u goes to $1/2$. Beyond this, for $1/2 \le u \le 1$, the $\beta\,(\sigma\,(u))$ term in (18) switches from the nth branch to the $(n+1)$st.

Correspondingly, at the nontrivial fixed point $u_* = 3/4$ of the step-scaling function, we see that $\beta(u_*)$ does *not* vanish for *any* of the branches of β. A typical RG trajectory in this chaotic case is shown here.

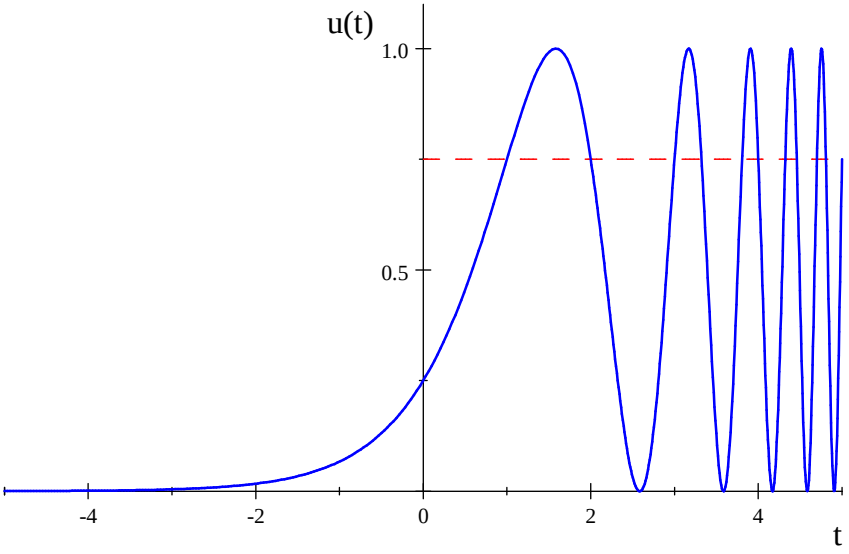

A trajectory with $u(0) = 1/4$, for the $s = 4$ multi-valued β function leading to chaotic evolution.

There is one highly unusual feature for the trajectory shown, as well as for all other trajectories for this example: The coupling actually goes to zero with increasing frequency but always "bounces back" to positive values. For a thorough discussion of this model using functional methods, in the context of classical mechanics for a chaotic dynamical system, see [8].

VII. DISCUSSION

In this paper we have elucidated, explored, and applied the underlying functional conjugacy structure of the renormalization group implicit in Gell-Mann and Low's finite renormalization group equation [14], structure which is normally overshadowed by local differential (Lie algebraic) features. We introduced methods to extract the links among fixed points of exemplary RG trajectories in section II. We applied some of these functional methods to obtain continuous flows from step-scaling functions utilized in lattice gauge theory, in section III. We explained in section IV how novel features could arise in general. We illustrated such features — including multi-valued β functions, limit cycles, and chaotic trajectories —

using toy models based on the logistic equation in section V.

The functional conjugacy core of the RG, (6), amounts to a solution by the method of characteristics, (12) et seq., so that scale changes are equivalent to variations of the initial coupling data. This controlling characteristic structure implies nonlocal associations in renormalization flows. In the large, the resulting functionally conjugate RG trajectories possess an elegant global mathematical consistency which sheds light on the flow of couplings in the presence of both UV and IR fixed points, and which also shows that trajectories may admit turning points, i.e. zeros of β functions where not all t derivatives of β vanish as a consequence of intricate branch structure. This latter possibility may lead to limit cycle or even chaotic behavior, as we have illustrated in some detail.

In this paper, models with only a single RG coupling flow have been considered . Extensions of the functional methods to models with more than one flowing coupling have yet to be carried out in complete detail. This is an area that warrants further exploration.

While we have not yet fully explored realistic quantum field theoretical models evincing *all* of the possibilities that we have discussed, we are confident that they do exist, at least for many of the features we have described. Presumably, the more exotic, *oscillatory* RG flows would only emerge in systems where the c-theorem [5, 28] (or its equivalent in higher dimensions [21]) does not hold [18, 27]. We would be most pleased to find in actual physical systems the full range of behavior illustrated by the toy models.

Acknowledgments

We thank Don Sinclair and Seth Quackenbush for comments on this work, and an anonymous referee for suggestions to improve the presentation. One of us (TC) thanks the CERN Theoretical Physics Group for its gracious hospitality and generous support, and the paragliders on the Salève for a convincing demonstration that interesting things can be done even in a crowded field. The numerical calculations and graphics in this paper were made using Maple®, Mathematica®, and MuPAD®. This work was supported in part by NSF Award 0855386, and in part by the U.S. Department of Energy, Division of High Energy Physics, under contract DE-AC02-06CH11357.

VIII. APPENDIX: NEWTONIAN TRAJECTORY AS A TRANSPORT OF DATA

Here we discuss analogies between RG flow and one-dimensional motion of a classical particle, thereby making contact with our previous work [7–9].

For fixed energy, E, the trajectory $x\left(t,x_0\right)$ of a particle moving in a one-dimensional potential, between turning points, depends only on time t and initial position $x_0 = x|_{t=0}$, since the initial momentum is fixed by E up to a choice of branch for $\sqrt{E-V\left(x\right)}$ (usually just an overall $\pm$ sign if V itself has only one branch). Thus

$$\int_{x_0}^{x(t,x_0)} \frac{dx}{v\left(x\right)} = t \ , \tag{83}$$

where $v\left(x\right)$ is the velocity profile along the trajectory. In this context it is clear that $v=0$ is not necessarily a fixed point. Rather more often it is a *turning point* of the motion.

Now, here's a simple technique that appears in Gell-Mann and Low (see Eq (B20), [14]): Differentiate (83) with respect to the initial position, regarding t and x_0 as independent variables. This gives

$$\frac{1}{v\left(x\left(t,x_0\right)\right)}\frac{\partial x\left(t,x_0\right)}{\partial x_0} - \frac{1}{v\left(x_0\right)} = 0 \ . \tag{84}$$

On the other hand, $v\left(x\left(t,x_0\right)\right) = \partial x\left(t,x_0\right)/\partial t$, so this last result is just

$$\frac{\partial x\left(t,x_0\right)}{\partial t} = v\left(x_0\right)\ \frac{\partial x\left(t,x_0\right)}{\partial x_0} \ . \tag{85}$$

That is to say, for want of a better name, this is a one-dimensional "Gell-Mann–Low transport equation" for $x\left(t,x_0\right)$. It is not quite "advection" [30] since that would have the form of a conservation law, namely, $\frac{\partial}{\partial t}f = \frac{\partial}{\partial x}\left(vf\right)$. The two types of transport are exactly the same only for constant v.

In fact, (85) is simpler than advection, with solutions of the FC form

$$x\left(t,x_0\right) = \Psi^{-1}\left(e^t \Psi\left(x_0\right)\right) \ , \tag{86}$$

for an appropriately defined Schröder function Ψ (although this terminology is *not* used in [14]) with inverse function Ψ^{-1}. By "appropriately defined" we mean,

$$v\left(x_0\right) = \Psi\left(x_0\right)/\Psi'\left(x_0\right) = \frac{1}{\left(\partial \ln \Psi\left(x_0\right)/\partial x_0\right)} \ , \tag{87}$$

hence Ψ is essentially just the exponentiated time to reach x from some reference point,

$$\Psi\left(x\right) = \Psi\left(x_{\rm ref}\right) \exp\left(\int_{x_{\rm ref}}^{x} \frac{dy}{v\left(y\right)}\right) \ . \tag{88}$$

Another way to express the result (86) is as a formal Taylor series in t, rewritten in terms of $v(x_0)$ and its derivatives through the use of (85). Thus

$$x(t,x_0) = \sum_{n=0}^{\infty} \frac{1}{n!}\, t^n\, \frac{\partial^n}{\partial \tau^n} x(\tau,x_0)\bigg|_{\tau=0} = \sum_{n=0}^{\infty} \frac{1}{n!}\, t^n \left(v(x_0)\ \frac{\partial}{\partial x_0} \right)^n x_0$$
$$= x_0 + t\ v(x_0) + \sum_{n=2}^{\infty} \frac{1}{n!}\, t^n \left(v(x_0)\ \frac{\partial}{\partial x_0} \right)^{n-1} v(x_0)\ . \tag{89}$$

(See Eq (B21) in [14].) If it is not already evident why this solution is formally the same as (86), then repeat some steps from the text and write the series in (89) as exponentiated operators.

$$x(t,x_0) = e^{t\frac{\partial}{\partial \tau}}\ x(\tau,x_0)\Big|_{\tau=0} = e^{t\ v(x_0)\ \frac{\partial}{\partial x_0}}\ x_0 = e^{t\ \frac{\partial}{\partial \ln \Psi(x_0)}}\ x_0\ , \tag{90}$$

where in the last step we have used (87). But now, $x_0 = \Psi^{-1}(\Psi(x_0)) = \Psi^{-1}(\exp(\ln \Psi(x_0)))$, so the last expression in (90) reduces to a translation of the variable $\ln(\Psi(x_0))$.

$$e^{t\ \frac{\partial}{\partial \ln \Psi(x_0)}}\ \Psi^{-1}(\exp(\ln \Psi(x_0))) = \Psi^{-1}(\exp(t + \ln \Psi(x_0))) = \Psi^{-1}\left(e^t \Psi(x_0)\right)\ . \tag{91}$$

Thus we recover (86) as an element of an abelian Lie group, given as usual by exponentiating an element of the underlying algebra — a symplectomorphism in the present context of classical mechanics.

IX. APPENDIX: A VARIABLE CHANGE AT A LATTICE FIXED POINT

For a supposed nontrivial fixed point, $u_* = 1/g_*^2$, determined by

$$\sigma(u_*) = u_*\ , \tag{92}$$

with $\beta(u_*) = 0$, we change variables in the lattice data formulas (42) and (43) of the text, by writing

$$\frac{1}{s} = (1+r)\, g_{0*}^2\ , \tag{93}$$

so that $r > 0$ for bare couplings g_0^2 *above* the fixed point value g_{0*}^2. Under this change of parameterization, we have

$$u = \frac{1}{(1+r)\, g_{0*}^2} \left(1 - \sum_{j=1}^{n} c_j\left(\ell\right) (1+r)^j \, g_{0*}^{2j} \right) = u_* + \sum_{j \geq 1} \mathfrak{a}_j\left(\ell\right) r^j \ , \tag{94}$$

$$u_* = \frac{1}{g_*^2} = \frac{1}{g_{0*}^2} \left(1 - \sum_{j \geq 1} c_j\left(\ell\right) g_{0*}^{2j} \right) \ . \tag{95}$$

$$\frac{du\left(s\right)}{ds} = \sum_{j \geq 0} \mathfrak{a}_j'\left(\ell\right) r^j \ , \quad \mathfrak{a}_j' = \left(j+1\right) \mathfrak{a}_{j+1} \frac{dr}{ds} \ , \quad \frac{dr}{ds} = -\frac{1}{g_{0*}^2 s^2} \ . \tag{96}$$

$$\mathfrak{a}_1 = \frac{1}{g_{0*}^2} \left(-1 - \sum_{j \geq 2} \left(j-1\right) c_j\left(\ell\right) g_{0*}^{2j} \right) \ , \quad \mathfrak{a}_2 = \frac{1}{g_{0*}^2} \left(1 - \frac{1}{2} \sum_{j \geq 3} \left(j-1\right)\left(j-2\right) c_j\left(\ell\right) g_{0*}^{2j} \right) \ , \tag{97}$$

$$\mathfrak{a}_{k<\max(n)} = \frac{1}{g_{0*}^2} \left(\left(-1\right)^k - \frac{1}{k!} \sum_{j \geq k+1} \left(j-1\right)\left(j-2\right) \cdots \left(j-k\right) c_j\left(\ell\right) g_{0*}^{2j} \right) \ , \quad \mathfrak{a}_k \underset{k \geq \max(n)}{=} \frac{\left(-1\right)^k}{g_{0*}^2} \ , \tag{98}$$

and therefore $\frac{1}{g_{0*}^2} \sum_{j=n+1}^{\infty} \left(-1\right)^j r^j = \frac{r^{n+1}}{(1+r) g_{0*}^2}$, as it should. Similarly

$$\sigma\left(u\right) = u_* + \sum_{j \geq 1} \mathfrak{a}_j\left(L\right) r^j \ , \quad \frac{d\sigma\left(u\left(s\right)\right)}{ds} = \sum_{j \geq 0} \mathfrak{a}_j'\left(L\right) r^j \ . \tag{99}$$

Discarding an overall $\frac{dr}{ds}$, the functional equation for the β function (44) is then

$$\left(\sum_{j \geq 0} \left(j+1\right) \mathfrak{a}_{j+1}\left(\ell\right) r^j \right) \beta \left(u_* + \sum_{k \geq 1} \mathfrak{a}_k\left(L\right) r^k \right) = \left(\sum_{j \geq 0} \left(j+1\right) \mathfrak{a}_{j+1}\left(L\right) r^j \right) \beta \left(u_* + \sum_{k \geq 1} \mathfrak{a}_k\left(\ell\right) r^k \right) \ . \tag{100}$$

Now it is straightforward albeit tedious to construct, up to an overall normalization, a series solution in r of this functional equation to obtain an expression for β near the fixed point. We shall *assume* u_* is a first-order zero of β.

$$\beta = \sum_{i=1}^{\min(n,N)} \mathfrak{b}_i r^i \ . \tag{101}$$

It would be nothing more than wishful thinking to carry the series approximation for β beyond that for either u or $\sigma\left(u\right)$.

For numerical work described in the text, we build the series solution to fourth order in r. Define $\mathfrak{a}_j\left(\ell\right) = \mathfrak{a}_j$, $\mathfrak{a}_j\left(L\right) = \mathfrak{A}_j$, and

$$\beta\left(u_* + w\right) = \mathfrak{b}_1 w + \mathfrak{b}_2 w^2 + \mathfrak{b}_3 w^3 + \mathfrak{b}_4 w^4 \ . \tag{102}$$

Then (100) gives

$$\begin{aligned}&\left(\mathfrak{a}_1+2\mathfrak{a}_2 r+3\mathfrak{a}_3 r^2+4\mathfrak{a}_4 r^3+5\mathfrak{a}_5 r^4\right)\ \beta\left(u_*+\mathfrak{A}_1 r+\mathfrak{A}_2 r^2+\mathfrak{A}_3 r^3+\mathfrak{A}_4 r^4\right)\\&=\left(\mathfrak{A}_1+2\mathfrak{A}_2 r+3\mathfrak{A}_3 r^2+4\mathfrak{A}_4 r^3+5\mathfrak{A}_5 r^4\right)\ \beta\left(u_*+\mathfrak{a}_1 r+\mathfrak{a}_2 r^2+\mathfrak{a}_3 r^3+\mathfrak{a}_4 r^4\right)\ .\end{aligned}\tag{103}$$

Now, we obviously cannot determine the overall normalization of β from the functional equation (100). This fact is why we find the same coefficient of r^1 on the LHS and RHS of this last equation, for any $\mathfrak{b}_1$. But higher powers of r give nontrivial information. For example, r^2 gives

$$\frac{\mathfrak{b}_2}{\mathfrak{b}_1}=\frac{\mathfrak{A}_1\mathfrak{a}_2-\mathfrak{A}_2\mathfrak{a}_1}{\mathfrak{A}_1\mathfrak{a}_1\left(\mathfrak{a}_1-\mathfrak{A}_1\right)}\ ,\tag{104}$$

while, r^3 gives

$$\frac{\mathfrak{b}_3}{\mathfrak{b}_1}=2\frac{\mathfrak{A}_2^2\mathfrak{a}_1^2-\mathfrak{A}_1^2\mathfrak{a}_2^2+\mathfrak{A}_1\mathfrak{a}_1\left(\mathfrak{A}_1\mathfrak{a}_3-\mathfrak{A}_3\mathfrak{a}_1\right)}{\mathfrak{A}_1^2\mathfrak{a}_1^2\left(\mathfrak{a}_1^2-\mathfrak{A}_1^2\right)}\ ,\tag{105}$$

and finally, r^4 gives the unwieldy expression

$$\frac{\mathfrak{b}_4}{\mathfrak{b}_1}=\frac{\left(\begin{array}{c}2\mathfrak{A}_1^3\mathfrak{A}_2\mathfrak{a}_1\mathfrak{a}_2^2+2\mathfrak{A}_1^2\mathfrak{A}_3\mathfrak{a}_1^3\mathfrak{a}_2-2\mathfrak{A}_1^3\mathfrak{A}_2\mathfrak{a}_1^2\mathfrak{a}_3-2\mathfrak{A}_1\mathfrak{A}_2^2\mathfrak{a}_1^3\mathfrak{a}_2-8\mathfrak{A}_1^3\mathfrak{a}_1^2\mathfrak{a}_2\mathfrak{a}_3+8\mathfrak{A}_1^2\mathfrak{A}_2\mathfrak{A}_3\mathfrak{a}_1^3\\-7\mathfrak{A}_1^4\mathfrak{a}_1\mathfrak{a}_2\mathfrak{a}_3+7\mathfrak{A}_1\mathfrak{A}_2\mathfrak{A}_3\mathfrak{a}_1^4+3\mathfrak{A}_1^4\mathfrak{a}_1^2\mathfrak{a}_4+3\mathfrak{A}_1^3\mathfrak{a}_1^3\mathfrak{a}_4-3\mathfrak{A}_1^3\mathfrak{A}_4\mathfrak{a}_1^3-3\mathfrak{A}_1^2\mathfrak{A}_4\mathfrak{a}_1^4\\+5\mathfrak{A}_1^3\mathfrak{a}_1\mathfrak{a}_2^3-5\mathfrak{A}_1\mathfrak{A}_2^3\mathfrak{a}_1^3+4\mathfrak{A}_1^4\mathfrak{a}_2^3-4\mathfrak{A}_2^3\mathfrak{a}_1^4+\mathfrak{A}_1^3\mathfrak{A}_3\mathfrak{a}_1^2\mathfrak{a}_2-\mathfrak{A}_1^2\mathfrak{A}_2\mathfrak{a}_1^3\mathfrak{a}_3-\mathfrak{A}_1^2\mathfrak{A}_2^2\mathfrak{a}_1^2\mathfrak{a}_2+\mathfrak{A}_1^2\mathfrak{A}_2\mathfrak{a}_1^2\mathfrak{a}_2^2\end{array}\right)}{\mathfrak{A}_1^3\mathfrak{a}_1^3\left(\mathfrak{a}_1^2-\mathfrak{A}_1^2\right)\left(\mathfrak{a}_1^2+\mathfrak{a}_1\mathfrak{A}_1+\mathfrak{A}_1^2\right)}\ .\tag{106}$$

And so it goes. We obtain $\mathfrak{b}_j/\mathfrak{b}_1$ as functions of the $\mathfrak{a}$s and $\mathfrak{A}$s. But again, it is overly ambitious to carry the series approximation for β beyond that for either u or $\sigma(u)$.

There remains only one coefficient to be determined, namely, $\mathfrak{b}_1$. This is given by

$$\mathfrak{b}_1=\ln\lambda=\ln\left(\frac{\mathfrak{a}_1(L)}{\mathfrak{a}_1(\ell)}\right)\ .\tag{107}$$

Although repetitious, a complete derivation of this result goes as follows. Setting the scale of t so that $u(t=1)=\sigma(u)$, Schröder's equation is, once again,

$$\Psi(\sigma(u))=\lambda\Psi(u)\ ,\tag{108}$$

and from $u(t)=\Psi^{-1}\left(\lambda^t\Psi(u)\right)$ with $\frac{du(t)}{dt}=\beta(u(t))$, we obtain $\beta(u(t))=(\ln\lambda)\,\Psi(u(t))/\Psi'(u(t))$. Now, at a fixed point $u_*=\sigma(u_*)$, with $\Psi(u_*)=0$, a series solution of (108) in powers of $(u-u_*)$ requires

$$\lambda=\left.\frac{d\sigma(u)}{du}\right|_{u=u_*}=\left.\frac{d\sigma/dr}{du/dr}\right|_{r=0}=\frac{\mathfrak{a}_1(L)}{\mathfrak{a}_1(\ell)}\ .\tag{109}$$

and also that $\beta(u) = (\ln\lambda)(u-u_*) + O\left((u-u_*)^2\right)$. Hence (107) is obtained. Alternatively, in terms of the original series involving the bare lattice coupling, we have

$$\lambda = \frac{1 + \sum_{j\geq 2}(j-1)\, c_j(L)\, g_{0*}^{2j}}{1 + \sum_{j\geq 2}(j-1)\, c_j(\ell)\, g_{0*}^{2j}} = \frac{u_* + \sum_{j\geq 1} j\ c_j(L)\, g_{0*}^{2j-1}}{u_* + \sum_{j\geq 1} j\ c_j(\ell)\, g_{0*}^{2j-1}}\ . \tag{110}$$

---

[1] T. Appelquist, G. T. Fleming, and E. T. Neil, "Lattice study of conformal behavior in SU(3) Yang-Mills theories" Phys. Rev. D **79**, 076010 (2009).

[2] E. Braaten, T. Curtright, and C. Zachos, "Torsion and Geometrostasis in Nonlinear Sigma Models" Nuclear Physics **B260**, 630-688 (1985).

[3] C. G. Callan, "Broken Scale Invariance in Scalar Field Theory" Phys. Rev. D **2**, 1541-1547 (1970).

[4] S. Caracciolo, R. G. Edwards, S. J. Ferreira, A. Pelissetto, and A. D. Sokal, "Extrapolating Monte Carlo Simulations to Infinite Volume: Finite-Size Scaling at $\xi/L \gg 1$" Phys. Rev. Lett. **74**, 2969-2972 (1995).

[5] J. Cardy, "The Ubiquitous 'c': from the Stefan-Boltzmann Law to Quantum Information." arXiv:1008.2331v3 [cond-mat.stat-mech].

[6] P. Collet and J. P. Eckmann, *Iterated Maps On The Interval As Dynamical Systems*, Birkhäuser (1980).

[7] T. Curtright and C. Zachos, "Evolution profiles and functional equations" J. Phys. A: Math. Theor. **42**, 485208 (2009). arXiv:0909.2424 [math-ph].

[8] T. Curtright and C. Zachos, "Chaotic Maps, Hamiltonian Flows, and Holographic Methods" J. Phys. A: Math. Theor. **43**, 445101 (2010). arXiv:1002.0104 [nlin.CD] .

[9] T. Curtright and A. Veitia, "Logistic map potentials" Phys. Lett. A arXiv:1005.5030 [math-ph].

[10] T. Curtright, "Potentials Unbounded Below" arXiv:1011.6056 [math-ph].

[11] R. L. Devaney, *An Introduction to Chaotic Dynamical Systems*, Addison-Wesley (1989).

[12] J. Ellis, I. Jack, D.R.T. Jones, M. Karliner, and M. A. Samuel, "Asymptotic Padé Approximant Predictions: up to Five Loops in QCD and SQCD" Phys. Rev. D **57** (1998) 2665-2675. arXiv:hep-ph/9710302.

[13] E. Gardi, G. Grunberg, and M. Karliner, "Can the QCD running coupling have a causal analyticity structure?" JHEP 9807:007 (1998). arXiv:hep-ph/9806462.

[14] M. Gell-Mann and F. E. Low, "Quantum Electrodynamics at Small Distances" Phys. Rev. **95**, 1300-1312 (1954).

[15] S. D. Głazek and K. G. Wilson, "Limit Cycles in Quantum Theories" Phys. Rev. Lett. **89**, 230401 (2002); Erratum, **92**, 139901 (2004).

[16] M. Kuczma, *Functional equations in a single variable*, Warsaw: P.W.N. (1968); M. Kuczma, B. Choczewski, and R. Ger, *Iterative Functional Equations*, Cambridge University Press (1990).

[17] A. LeClair, J. M. Román, and G. Sierra, "Russian Doll Renormalization Group and Superconductivity" Phys. Rev. B **69** 20505 (2004) arXiv:cond-mat/0211338; "Russian Doll Renormalization Group, Kosterlitz-Thouless Flows, and the Cyclic sine-Gordon model" Nucl. Phys. **B675** 584-606 (2003) arXiv:hep-th/0301042; "Log-periodic behavior of finite size effects in field theories with RG limit cycles" Nucl. Phys. **B700** 407-435 (2004) arXiv:hep-th/0312141.

[18] A. LeClair and G. Sierra "Renormalization group limit-cycles and field theories for elliptic S-matrices" J. Stat. Mech. 0408:P004 (2004) arXiv:hep-th/0403178.

[19] T. D. Lee, *Particle Physics and Introduction to Field Theory*, Harwood Academic (1981), pp 458-462.

[20] M. Lüscher, P. Weisz, and U. Wolff, "A Numerical Method to Compute the Running Coupling in Asymptotically Free Theories" Nucl. Phys. **B359**, 221-243 (1991).

[21] R. C. Myers and A. Sinha, "Seeing a c-theorem with holography." arXiv:1006.1263v2 [hep-th].

[22] T. A. Ryttov and F. Sannino, "Supersymmetry inspired QCD beta function" Phys. Rev. D **78**, 065001 (2008).

[23] E. Schröder, "Über iterirte Funktionen" *Math. Ann.* **3**, 296-322 (1870).

[24] E. C. G. Stueckelberg and A. Petermann, "The normalization group in quantum theory" Helv. Phys. Acta **24** (1951) 317-319; "La normalisation des constantes dans la théorie des quanta" Helv. Phys. Acta **26** (1953) 499-520.

[25] K. Symanzik, "Small Distance Behaviour in Field Theory and Power Counting" Commun. math. Phys. **18**, 227-246 (1970); "Small-Distance-Behaviour Analysis and Wilson Expansions" Commun. math. Phys. **23**, 49-86 (1971).

[26] K. G. Wilson, "Renormalization Group and Strong Interactions" Phys. Rev. D **3**, 1818-1846

(1971).

[27] K. G. Wilson and S. D. Głazek, "Universality, marginal operators, and limit cycles" Phys. Rev. B **69**, 094304 (2004).

[28] A. B. Zamolodchikov, "'Irreversibility' of the Flux of the Renormalization Group in a 2-D Field Theory" JETP Lett. **43**, 730-732 (1986).

[29] Given any solution $\Psi(u)$ of Schröder's functional equation, there exists an associated infinite family of solutions of the form $\Psi(u) \times P(\ln \Psi(u))$ where P is *any* periodic function of period $\ln \lambda$. The so-called *principal solutions* that we construct by series methods in this paper are always chosen to have $P = 1$. Otherwise, we would be faced with the ambiguity of a family of Callan-Symanzik functions: $\beta(u; P) = \beta(u; 1) / \left(1 + (\ln P)'\right)$. These would correspond to (rather peculiar) redefinitions of the coupling: $\mathfrak{u}(u) = \int^u \frac{du}{1+(\ln P)'}$.

[30] Sidney Coleman, a student of Gell-Mann, discusses renormalization group flows in one of his Erice lectures, using an analogy with the advection of bacteria moving down a pipe. See §4.1 of Chapter 3 ("Dilatations") in S. Coleman, *Aspects of symmetry*, Cambridge University Press (1985).

[31] Higher-order renormalization group differential equations have been encountered in models coupled to quantum gravity in two dimensions. We thank S. R. Das for bringing this to our attention. See S. R. Das, S. Naik, and S. R. Wadia, "Quantization of the Liouville Mode and String Theory" Mod. Phys. Lett. **A4** (1989) 1033-1041; S. R. Das, A. Dhar, and S. R. Wadia, "Critical Behavior in Two-Dimensional Quantum Gravity and Equations of Motion of the String" Mod. Phys. Lett. **A5** (1990) 799-813; A. M. Polyakov, "Singular States in 2D Quantum Gravity" pp 175-189 in *Two Dimensional Quantum Gravity and Random Surfaces,* proceedings of the Jerusalem Winter School for Theoretical Physics, 27 Dec 1990-4 Jan 1991, D. J. Gross, T.Piran, and S. Weinberg (ed), World Scientific (1992).